

**DESIGN AND FABRICATION OF AN INTEGRATED
MICROCONTROLLER SECURITY SYSTEM**

SAKAYO MUOKI

MASTER OF SCIENCE

(Physics)

**JOMO KENYATTA UNIVERSITY
OF
AGRICULTURE AND TECHNOLOGY**

2023

**Design and Fabrication of an Integrated Microcontroller Security
System**

Sakayo Muoki

**A Thesis Submitted in Partial Fulfillment of the Requirements for the
Degree of Master of Science in Physics of the Jomo Kenyatta
University of Agriculture and Technology**

2023

DECLARATION

This thesis is my original work and has not been presented for a degree in any other University

Signature..... Date.....

Sakayo Muoki

This thesis has been submitted for examination with our approval as the University Supervisors

Signature..... Date.....

Prof. Joseph N. Mutuku, PhD
JKUAT, Kenya

Signature..... Date.....

Dr. James. M. Ngaruiya, PhD
JKUAT, Kenya

DEDICATION

This thesis is dedicated to my parents Mr. and Mrs. Joseph Kavoi for their inspiration in my world of academics from my tender age. They have really modelled and triggered my thoughts throughout. They have made me realize the potential I have and I will always be indebted to you. In addition, the late Dr. Nicholas Muthama Mutua, had been more than a mentor. I lack precious words to use, but may you continue resting in peace.

ACKNOWLEDGEMENT

My true and sincere appreciation goes to all those who contributed towards the achievement of this research work. I appreciate Prof. Mutuku J.N. and Dr. Ngaruiya J.M. under whom I had the special honor to be instructed. Truly grateful I am to them for their guidance in research development and their socializing me in the art of scientific scholarship.

I appreciate so much my beloved wife for her continued strong inspirational support, encouragement and patience. My special thanks to the late Dr. Mutua and Dr. Kiroe for moral support and encouragement throughout. Words cannot adequately express how much I am indebted to the staff in the department of Physics and Chemistry at large for their great deal of contributions to this research activity.

TABLE OF CONTENTS

DECLARATION.....	ii
DEDICATION.....	iii
ACKNOWLEDGEMENT	iv
TABLE OF CONTENTS.....	v
LIST OF TABLES	ix
LIST OF FIGURES	x
LIST OF PLATES	xiii
LIST OF APPENDICES	xiv
LIST OF SYMBOLS	xv
ABBREVIATIONS AND ACRONYMS.....	xvii
ABSTRACT.....	xix
CHAPTER ONE	1
INTRODUCTION AND LITERATURE REVIEW	1
1.1 Introduction	1
1.2 Literature Review	2

1.3 Statement of the problem	12
1.4 Justification	12
1.5 Research hypothesis	13
1.6 Research objectives	13
1.6.1 General objective	13
1.6.2 Specific Objectives	13
CHAPTER TWO	14
MATERIALS AND METHODS	14
2.1 Introduction	14
2.2 Design methodology.....	14
2.3 The hardware design modules of the proposed microcontroller security system. .	15
2.3.1 Gas sensor module	16
2.3.2 Design and instrumentation of simulation circuit of the MQ-4 gas sensor module.....	18
2.3.3 Heating of MQ-4 gas sensor for sensitivity adjustment	18
2.3.4 Preparation of methanol solution.....	19
2.2.5 Experimental set up for gas sensor module	21
2.3 Infrared Sensor module	22

2.3.1 Introduction.....	22
2.3.2 The PIR Sensor	23
2.3.3 How PIR Work	23
2.3.4 Detecting area coverage.....	24
2.3.5 PIR sensor characteristics for objects at different distances and heights	25
2.4 Temperature measurement with LM35 temperature sensor	26
2.4.1 LM35 Temperature Sensor	26
2.4.2 ADC0831 Analogue-to-digital Converter	27
2.4.3 Process of Measurement with LM35 Temperature Sensor.....	28
2.5 Arduino Uno Microcontroller.....	30
2.6 LCD display	32
2.7 Buzzer.....	32
2.8 Programmable peripheral interface	32
2.9 GSM modem	32
2.10 System circuit diagram of the Hardware design.....	32
2.11 System circuit diagram of the Software design.....	34
CHAPTER THREE	35
RESULTS AND DISCUSSION	35

3.1 Introduction	35
3.2 Analysis of MQ-4 Gas Sensor in Ideal Situation	35
3.2 Calibration of the MQ-4 gas sensor using methanol.	37
3.3 Infrared sensor results	43
3.4 Fire/Temperature Sensor	56
3.5 The Integrated Microcontroller Security System	57
CHAPTER FOUR.....	62
CONCLUSIONS AND RECOMMENDATIONS.....	62
4.1 Conclusion.....	62
4.3 Recommendations	62
REFERENCES.....	64
APPENDICES	67

LIST OF TABLES

Table 1.1: The structural and molecular formula for methane, ethane, propane and butane	8
Table 2.1: Datasheet of sensitivity characteristics of MQ-4 gas sensor (www.hwsensor.com).....	17
Table 2.2: Attribute Features of Experiment Object	25

LIST OF FIGURES

Figure 1.1: (a) Structure of methane molecule, (b) Illustration of bonding angles in methane molecule (Walker, 2008).....	9
Figure 2.1: Block diagram of modules and their interconnection.....	14
Figure 2.2: A schematic test circuit of MQ-4 gas sensor.....	16
Figure 2.3: Simplified circuit of MQ-4 gas sensor. R_L and R_S resistors are connected in series.	17
Figure 2.4: Simulation circuit of finding optimum resistance	18
Figure 2.5: Flowchart diagram of the MQ-4 sensor sensitivity adjustment process.....	21
Figure 2.6: Ideal sensitivity characteristics of MQ-4 gas sensor (Pololu robotics and electronics).....	22
Figure 2.7: Internal schematic diagram of passive infrared sensor.....	23
Figure 2.8: Schematic diagram Illustrating PIR functioning	24
Figure 2.9: Basic Centigrade Temperature Sensors.....	27
Figure 2.10: A schematic diagram of the ADC0831 ADC	28
Figure 2.11: (a) Pin out diagram of LM35 temperature sensor (b): Schematic diagram of LM35 temperature sensor connected to ADC0831 converter	29
Figure 2.12: Pin diagram of Arduino Uno (Rev3) microcontroller	30
Figure 2.13: Circuit diagram of the Arduino Uno based security system	33
Figure 2.14: Flowchart depicting functioning of the security system.....	34

Figure 3.1: A graph of voltage, V_{RL} (mV) versus concentration (ppm) of methanol for the MQ-4 gas sensor for methanol under ideal conditions.	36
Figure 3.2: Graph of output voltage (mV) versus concentration of methanol (ppm) in different exposure-time after 24 hours of heating MQ-4 gas sensor.	38
Figure 3.3: Graph of output voltage (mV) versus concentration of methanol (ppm) in different exposure-times after 2 days of heating MQ-4 gas sensor.	39
Figure 3.4: Graph of output voltage (mV) versus concentration of methanol (ppm) in different exposure-times after 3 days of heating MQ-4 gas sensor.	40
Figure 3.5: Graph of output voltage (mV) versus concentration of methanol (ppm) in different exposure-times after 4 days of heating MQ-4 gas sensor.	41
Figure 3.6: Graph of output voltage (mV) versus concentration of methanol (ppm) in different exposure-times after 5 days of heating MQ-4 gas sensor.	42
Figure 3.7: The root mean square value of detector voltage at different distances at different walking speed for PIR placed 0.5 m above the ground	44
Figure 3.8: The root mean square value of detector voltage at different distances and different walking speed for PIR placed 1.0 m above the ground.	45
Figure 3.9: The root mean square value of detector voltage at different distances at different walking speed for PIR placed 1.5 m above the ground	46
Figure 3.10: The root mean square value of detector voltage at different distances at different walking speed for PIR placed 1.8 m above the ground	47
Figure 3.11: Detector sensitivity at different angles when the subject walked towards the detector at different walking speeds sensor placed at 0.5 m above the ground	48

Figure 3.12: Detector sensitivity at different angles when the subject walked towards the detector at different walking speeds sensor placed at 1 m above the ground.49

Figure 3.13: Detector sensitivity at different angles when the subject walked towards the detector at different walking speeds sensor placed at 1.5 m.50

Figure 3.14: Detector sensitivity at different angles when the subject walked towards the detector at different walking speeds sensor placed at 1.8 m.51

Figure 3.15: Detector sensitivity at different angles when the subject walked away from PIR sensor at different angles with the PIR sensor positioned 0.5 m above the ground.52

Figure 3.16: Detector sensitivity at different angles when the subject walked away from PIR sensor at different angles with the PIR sensor positioned 1.0 m above the ground.53

Figure 3.17: Detector sensitivity at different angles when the subject walked away from PIR sensor at different angles with the PIR sensor positioned 1.5 m above the ground.54

Figure 3.18: Detector sensitivity at different angles when the subject walked away from PIR sensor at different angles with the PIR sensor positioned 1.8 m above the ground.55

Figure 3.19: A graph of Temperature (0C) against Output voltage (mV) of the LM3 temperature Sensor.56

LIST OF PLATES

Plate 2.1: Diagram showing how MQ-4 was heated up.	19
Plate 3.1: The experimental arrangement set up to measure voltage drop across resistor R_L when the MQ-4 gas sensor is exposed to different concentrations of methanol.	37
Plate 3.2: MQ-4 gas sensor and the PIR sensor connected to the Arduino UNO.	57
Plate 3.3: The Arduino UNO security system connected to the power supply.	58
Plate 3.4: The LCD display when the system under normal conditions of temperature and gas concentration.	59
Plate 3.5: a. The temperature is above 40 °C and the buzzer goes on and the red signal light goes on continuously to indicate there is a danger. b. The short message of fire sent to home owner mobile phone	60

LIST OF APPENDICES

Appendix I: The program for running the software for the integrated Arduino microcontroller based security system.	67
Appendix II: List of Publications	71

LIST OF SYMBOLS

c	speed of light
E	energy
h	Planck's constant
H_c	the heat of combustion of the fuel
k	Boltzmann constant
M_C	the fuel mass consumed per unit area
T	Absolute temperature
ε	emissivity
λ	wavelength
σ	Stefan-Boltzmann constant
i_{lim}	diffusion limited current in amperes
F	Faraday constant (96,500 coulombs)
A	reaction interfacial area
n	number of electrons per mole reactant,
δ	diffusion path length,
C	gas concentration in moles/cm ³ ,
D	gas diffusion constant

M	mass
ρ	Density
V	Volume
R_s	sensing resistance,
R_L	loading resistance,
V_{RL}	loading voltage
V_{CC}	supply voltage

ABBREVIATIONS AND ACRONYMS

AC	Alternating Current
CPU	Central Processing Unit
EEPROM	Electrically Erasable Programmable Read Only Memory
FET	Field Effect Transistor
GSM	Global System for Mobile communications
IDS	Intruder Detection System
IC	Integrated circuit
I/O	Input/output
IR	Infra-Red
JFET	Junction gate field-effect transistor
LCD	Liquid Crystal Display
LED	Light Emitting Diode
LM	Linear Monolithic
MO	Molecular Orbital
MQ-4	Methane and Natural Gas 4 th Series sensor.
MSA	Mine Safety Appliances
NSA	National Semiconductor Application

PIN	Personal Identification Number
PIR	Pyro-electric Infrared
PPM	Parts per Million
RAM	Random Access Memory
ROM	Read Only Memory
SIM	Subscriber Identity Module
SMS	Short Message Service
SnO₂	Tin (IV) Oxide

ABSTRACT

Ubiquitous insecurity brought about by terrorism and advances in human development and technology are significantly on rise. People now live in more advanced homes with facilities that make life more comfortable but also are sources of insecurity. Coupling with advances in science and technology, security systems have been developed. However, apart from monitoring and relying information, more precise information in terms of characterization, sensitivity and proximity appropriation of the sensors is not fully exploited. This research project upholds on the development of Arduino UNO microcontroller based integrated home security system. It involves the characterization of MQ-4 gas sensor using the theory of diffusion concentration so as to detect the leakage of cooking gas and give feedback. In addition, unlike the closed circuit television (CCTV) which can only record the video without alerting the owner passive infrared (PIR) motion sensor will give the proximity of the intruder and increase the sensitivity for detecting intruders. The characterization of the MQ-4 gas sensor using theory of diffusion concentration uses the standard prepared alcohol. The characterization of the LM-35 temperature sensor through voltage variation was also investigated. The interfacing of the sensors and the other electronic components such as buzzer, global system for mobile communications (GSM), subscriber identity module (SIM 900) and liquid crystal display (LCD) were integrated and controlled by the Arduino UNO. The Arduino UNO controls all communication signals between these electronic instruments in this system through a developed software program. The results of the system and its sensors show that the proposed system successfully detects the cooking gas leakage, intruder intrusion and fire outbreak.

CHAPTER ONE

INTRODUCTION AND LITERATURE REVIEW

1.1 Introduction

Security is literally a means or method by which something is secured through a system of interworking components and devices. Home security systems are networks of integrated electronic devices working together with a central control panel to protect against burglars and other potential home intruders, gas leakage and fire outbreak (Celeste Tholen, 2021)

The need to secure our homes, commercial complexes, industries and other related properties is of much concern. A home security system should provide security and safety features for a home by alarming the residents from natural and accidental dangers such as; fire, flooding, theft, invading animals and leakage of cooking gas. Considering the high rate of crime and insecurity, there is an urgent need to design a security system that takes proper measure to prevent intrusion, unwanted and unauthorized user(s).

Microcontrollers play a very vital role in the development and implementation of automation technology. According to Lakra (2015) automation is the process of controlling system and information to decrease the need of human participation and increase accuracy. Home automation represents the idea of controlling of home appliances in an integrated system. This includes control of heating, ventilation, air-conditioning, security, and other appliances. Several sensors i.e. detectors for temperature/fire gas and motion are used for this home security system. These sensors use the input signal to control home appliances. The implementation of a unified connectivity between devices and the main controller in cost effective way is very decisive hence the need to design and fabricate a simple microcontroller based home security monitoring system.

The design of the monitoring system has been influenced by today's technological advancements. There are different kinds of home security systems, but the basic types are wireless security alarms, microcomputer based security system, motion sensor, access control gates and wireless global service for mobile (GSM) based communication system.

A wireless security alarm security system sends an alarm to the property owner before intruders get in and summons help immediately. The microcomputer based security system senses the presence of an intruder and alerts the user on the obstruction detected and it also displays the position of the intruder on a screen. A motion sensor detects a change in infrared light intensity and produces a signal which is used to raise an alarm. This makes it hard for the intruder to get on the secured property by surrounding the home with a high fence and installing an automatic access control gate. It also gives specific points of entry onto the property and one can monitor the entry points from inside. Wireless GSM communication system provide security from natural, incidental, intended, unintended accidental and human made problems by continuously monitoring homes with different sensory systems like motion, smoke, gas, temperature, glass break or door break detectors and fire alarm systems, (Lakra,2015).

1.2 Literature Review

Many types of home security systems have been developed. Home or office automation is the control of any or all electrical devices in our homes or offices (Kaur, 2010). This is one of the most exciting developments in technology that has come along in decades. There are hundreds of products available today that allow the control of devices automatically either by remote control or bio-data such as face, prints etc. Most of these systems are based on microprocessors or microcontrollers (Kaur, 2010). Microcontroller is designed for a very specific task to control a particular system.

Some microprocessor and microcontroller based systems have been designed to control the opening and closing of doors and gates and alert the owner in case of an intruder and

fire outbreaks. Lau and Choo (1989) designed a microprocessor based gate security system. This system automatically controlled the visitors at the gate by use of a password. The system design used microprocessor based card which used software to control the password keys. There were four modules which included data module, management mode, tenant mode and the alarm module

Gwagwa (2010) worked on a design and construction of a microcontroller-based mains switch control system. The system automatically controlled alternating current (AC) loads connected to it through a serial port interface. In addition, the switch control system can range from simple control of lights to switch ON and OFF industrial electrical devices through a computer interface.

Another design and implementation of a smart home enabled the control of home electronic devices remotely and produced an alert on intrusion or movement around the restricted premises (Luitel, 2013). The devices were controlled by a mobile phone using the short message service (SMS) and alerts were received as SMS message describing the activity occurring around the premises.

From research conducted by Visa and Victor (2012), it was found that majority of the existing car security systems use only alarm, and do not send text message to the car owner let alone demobilizing the car. They designed a microcontroller based car anti-theft security system using GSM network with text message as feedback. The need for this arose due to the increasing rate at which parked cars are stolen. With this design a parked car is monitored irrespective of where it is parked, provided there is GSM network coverage. Diarah *et al.*, (2014), describes a microcontroller code locking systems with alarm. Code based locking system is best suited for most applications because of its simplicity and reliability. Since such a system is always resident in the area being protected, there are fewer chances of security breaches unlike the keycard lock system in which the access card can fall into unauthorized hands. Furthermore, in the issue of maintenance, the access code can easily be changed at will with lesser cost unlike the keycard system where a new set of access cards are required.

Nwankwo and Nsionu, (2013) presented both design and the implementation of a microcontroller based security door system using a mobile phone and a computer set. The security door could either receive command through the mobile phone or through the computer system configured to output data through the parallel port.

Hui, (2013) worked on a microcontroller-based lock using color security code. This microcontroller based lock used the color sequence code as password to unlock the system. The major drawback of this color code is the insensitivity of button since some of the buttons have to be pressed using more force causing delay in the time for the button scanning, data logging and mobile communication as this lock system used only stored data in form of password. As this lock only operated with the random colour, it would not suit the users who suffer from colour blindness. Another microcontroller based home security system designed by Agarwal and Nayak (2012), utilized wireless alerts using radio frequency (RF) signals as communication standards.

a. Intruder detection

In most of the security systems, detectors are used to achieve a secured home or office. Passive infrared detector is widely used in presence detectors as a means of human detection (Moghavvemi and Seng (2004). They worked on application of pyro electric infrared sensor (PIR) and the application of processing algorithm in handling sensor information so as to provide real time occupancy map on computer. The PIR sensor was used to detect the presence of human in a protected room. Wireless communications network using frequency modulation technique was developed to handle data transmission through the air. The personal computer played a significant role in providing the intelligent centralized controls of the entire system. A software package was developed for visual display, control mechanism configuration, and embedded server-client application. Alkhatami *et al.*, (2015), researched on various border intrusions detection systems with emphasis on wireless sensor detection method. The system detects human and non-human intruders such as objects and animals. Thus, their

study aimed at ascertaining the intruder crossing a specified border or perimeter under surveillance before raising an alarm.

Kumar, (2013) in his research developed an Arduino[®] based wireless intrusion detection using IR sensor and GSM. This intrusion detection system (IDS) involves a software and hardware tool used to detect unauthorized access of a computer system or network. A wireless IDS performs this task exclusively for the wireless network through sensor controlling with different workstations via internet. An IDS usually performs this task in one of two ways, with either signature-based or anomaly based detection. Almost every IDS today is at least in part signature-based. Attacks, which are unwanted intrusions, and their tools usually have a unique signature that can be detected and/or found. This means that known attacks can be detected by looking for these signatures. The drawback with these systems is that they are easy to fool and can only detect attacks for which it has a signature. These are not often implemented, mostly because of the high amount of false alarms. An anomaly-based system develops a baseline of what it considers normal traffic. Any time it detects traffic which deviates from what it considers normal an alert is generated. The advantage is that it can catch many attacks that are new or unknown and that would never be seen by signature-based IDS (Kumar, 2013).

b. Gas leakage detection

MQ-4 gas sensor is made of porous SnO₂ films with a high surface to volume ratio. During operation the gas sensing material is heated. The exact fundamental mechanisms that cause a gas response are still controversial, but essentially trapping of electrons at adsorbed molecules and band bending induced by these charged molecules are responsible for a change in conductivity. When a molecule adsorbs at the surface electrons can be transferred to this molecule if the lowest lying unoccupied molecular orbitals of the adsorbate complex lie below the Fermi level (acceptor levels) of the solid and vice versa electrons are donated to the solid if the highest occupied orbitals lie above the Fermi-level of the solid (donor levels). Thus molecular adsorption may result in a net charge at the surface causing an electric field. This electrostatic field causes a bending of

the energy bands in the solid. A negative surface charge bends the bands upward, i.e. pushes the Fermi level into the band gap of the solid, effectively reducing the charge carrier concentration and resulting in an electron depletion zone. Depleting electrons causes a positive space charge region that compensates for the negative surface charge. The charge density distribution in the depletion zone can be determined by solving the one dimensional Poisson equation:

$$p(z) = e[p(z) - n(z) + D^+ - A^-] = -\epsilon_r \epsilon_0 d^{-2} V/dz^2 \dots\dots\dots 1.1$$

Where e is the elementary charge, p and n are the charge carrier densities, i.e. the number of holes and electrons, and D⁺ and A are the densities of singly charged donors and acceptors and ε_r is the dielectric constant of the material. Charge neutrality of the system invokes that integration of the charge q(z) over the entire volume has to be equal to the surface charge trapped in the adsorbed molecule. Generally, the Poisson equation cannot be solved analytically, but for the simplest case with negligible acceptor and hole concentration (n-type semiconductor) and complete ionization of the donors, i.e. D⁺(z) = D⁺ = constant., the Poisson equation can be rewritten as

$$e[-n(z) + D^+] = \epsilon_r \epsilon_0 \frac{d^2 V}{dz^2} \dots\dots\dots 1.2$$

Abrupt transition of the charges with n(z) = D⁺ in the bulk and n(z) = 0 in the space charge region makes the first integration of Equation 4.2 straight forward and yields a linear relationship of the electric field E:

$$E(z) = \frac{dV}{dz} = \frac{eD^+(z-D)}{\epsilon_r \epsilon_0} \dots\dots\dots 1.3$$

Where D is the Debye length or depth of the space charge region. Charge neutrality of the system requires that the space charge is equal to the surface charge, i.e.

$$D^+ \cdot D = N_s \dots\dots\dots 1.4$$

Where N_s is the number of elementary surface charges (singly charged adsorbed molecules) per unit area. To find the variation of the potential in the space charge region the second integration of the Poisson equation is calculated:

$$V = eD^+ \frac{(z - D)^2}{2\epsilon_r \epsilon_0} \dots\dots\dots 1.5$$

If we define the potential to be zero within the bulk $V(z > D) = 0$ and by using equation 4.5 to eliminate D the surface ($z = 0$) potential can be written as:

$$V_s = \frac{eD^+ + D^2}{2\epsilon_r \epsilon_0} = \frac{eN_s^2}{2\epsilon_r \epsilon_0 D^+} \dots\dots\dots 1.6$$

As a consequence of the charge carrier depletion zone in the presence of surface charges the sheet conductivity r of the surface is altered. This change in conductivity is commonly used as the signal in gas sensing devices and hence accounting of the shift of the heating curves.

A gas detector detects the presence of gases in an area, often as part of a safety system. A gas detector can sound an alarm to operators in the area where the leak is occurring, giving them the opportunity to react to the leakage. Several authors have designed gas detection systems (Williams and Keeling, 1998; Pregeij and Mozetic, 1999; Ichoku and Kaufman, 2005; Priya *et al.*, 2014). A gas leak detector circuit that detects the leakage of liquid petroleum gas (LPG) and alerts the user through audio-visual indications has been constructed (Priya *et al.*, 2014). Further, the Mine Safety Appliances (MSA) Company designed a ultrasonic gas leak detectors based on robust microphone technology that

detect leaks by sensing the distinct high frequency ultrasound emitted by all high pressure gas leaks (www.msasafety.com accessed on 17th October 2021).

Murvy and Silea, (2012) in their work, identified a state-of-the-art method in leak detection. They evaluated the capabilities of the techniques in order to identify the advantages and disadvantages of using the leak detection solution.

In general, a molecule with N atoms has $3N - 6$ normal modes of vibration, but a linear molecule has $3N - 5$ such modes, as rotation about its molecular axis cannot be observed (Walker, 2008).

Table 1.1 shows the first four elements of alkane group of organic compounds and their formulas. They are mostly used as fuels hence form high percentage of natural gas. Cooking gas mostly consists of methane gas. Methane molecule consists of one carbon and four hydrogen atoms (CH_4). In methane C-atom is sp^3 -hybridized. One s-orbital and three p-orbitals ($2p_x$, $2p_y$, $2p_z$) of carbon atom undergo sp^3 -hybridization to produce four sp^3 -hybrid orbitals. These sp^3 -hybrid orbitals are 109.5° apart. Each sp^3 -hybrid orbital overlaps 1s-orbital of H-atoms. In this way four s-bonds are produced between C and four H-atoms.

Table 1.1: The structural and molecular formula for methane, ethane, propane and butane

Number of carbon atoms	Name	Molecular Formula	Structural Formula
1	Methane	CH_4	CH_4
2	Ethane	C_2H_6	CH_3CH_3
3	Propane	C_3H_8	$\text{CH}_3\text{CH}_2\text{CH}_3$
4	Butane	C_4H_{10}	$\text{CH}_3\text{CH}_2\text{CH}_2\text{CH}_3$

The structure of a methane gas molecule is shown in Figure 1.2 (a and b).

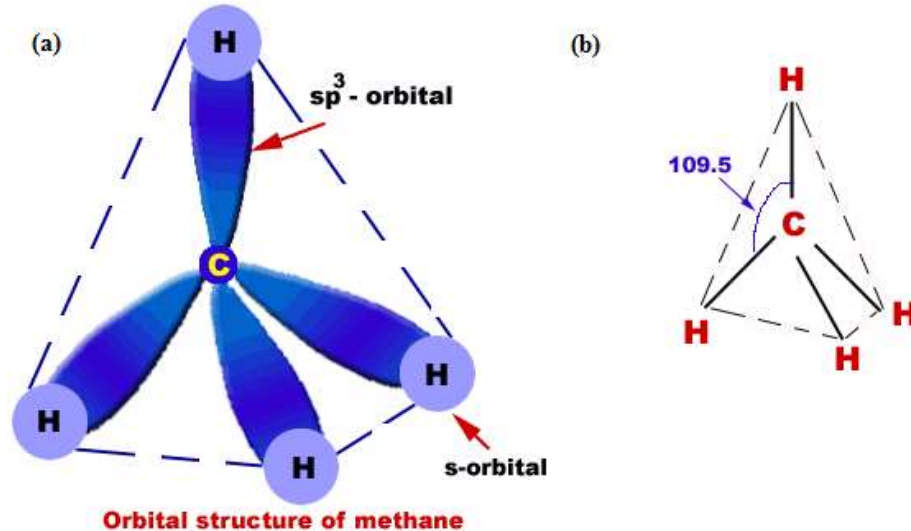


Figure 1.1: (a) Structure of methane molecule, (b) Illustration of bonding angles in methane molecule (Walker, 2008).

It is tetrahedral in structure, in which carbon is the central atom and four H-atoms are surrounding it in three-dimensions. The structure of any molecule is unique for all molecules. Due to this uniqueness the infrared radiation interacts with the molecules with different absorptions and transmittances.

The absorption of the infrared by these gases will be set as the values within which the outputs will be active. This is described through the diffusion principle. The MQ-4 gas sensor is an electrochemical gas detector operating under diffusion controlled conditions. Sensitive material of MQ-4 gas sensor is tin (IV) oxide (SnO_2) which has lower conductivity in clean air. When the target combustible gas exist, the sensor's conductivity is higher along with the gas concentration rising. The principle of operation is described as follows: gas molecules from the sample are adsorbed on an electro catalytic sensing electrode, after passing through a diffusion medium, and are electrochemically reacted at an appropriate sensing electrode potential. This reaction generates an electric current directly proportional to the gas concentration. This current is converted to a voltage for meter or recorder I readout.

The diffusion limited current, i_{lim} , is directly proportional to the gas concentration according to the simplified equation 1.7 (Wang, 1999).

$$i_{lim} = \frac{nFADC}{\delta} \dots\dots\dots 1.7$$

where i_{lim} is the diffusion limited current in amps, F is the Faraday constant (96,500 coulombs), A is the reaction interfacial area in cm^2 , n is the number of electrons per mole reactant, δ is the diffusion path length, C is the gas concentration in moles/ cm^3 , and D is the gas diffusion constant, representing the product of the permeability and solubility coefficients of the gas in the diffusion medium.

An external voltage bias maintains a constant potential on the sensing electrode, relative to a non-polarizable reference counter electrode in the two-electrode inter scan sensor. Non-polarizable means that the counter electrode can sustain a current flow without suffering a change in potential. Thus, the counter electrode acts also as a reference electrode, eliminating the need for a third electrode and a feedback circuit, as would be required for sensors using a polarizable air counter electrode.

c. Fire /temperature detection

According to National Semiconductor application (NSA) (2016) most commonly-used electrical temperature sensors are difficult to apply. For example, thermocouples have low output levels and require cold junction compensation and thermistors have nonlinear outputs. In addition, the outputs of these sensors are not linearly proportional to any temperature scale. Early monolithic sensors, such as the LM3911, LM134 and LM135, overcame many of these difficulties, but their outputs are related to the Kelvin temperature scale rather than the more popular Celsius and Fahrenheit scales. Fortunately, in 1983 two integrated circuit (I.C.), the LM34 Precision Fahrenheit Temperature Sensor and the LM35 Precision Celsius Temperature Sensor, were introduced. This application note will discuss the LM35, but with the proper scaling

factors can easily be adapted to the LM35. The LM35 has an output of linearity of +10mV/°C with non-linearity of only ±¼°C over a temperature range of –55°C to 150° and is accurate to within 0.5°C (at 25°C typically at room temperature). The LM35’s low output impedance and linear output characteristic make interfacing with readout or control circuitry easy. An inherent strength of the LM35 over other currently available temperature sensors is that it is not as susceptible to large errors in its output from low level leakage currents to readout or control circuitry especially easy. The device is used with single power supplies, or with plus and minus supplies. As the LM35 device draws only 60 µA from the supply and has very low self-heating of less than 0.1°C in still air. The LM35 device is rated to operate over a –55°C to 150°C temperature range, while the LM35C device is rated for a –40°C to 110°C range (–10° with improved accuracy).

Kaushik and Celler, (2006) in their paper states that all objects constantly exchange thermal energy in the form of electromagnetic radiations with their surroundings. The characteristics of the radiations depend on the object and its surroundings’ absolute temperature.

Human bodies also emit radiation and the wavelength of these radiations can be calculated using Wien’s law which is given in equation,

$$\lambda_{\max}(cm) = \frac{2898}{Temperature(K)} \dots\dots\dots 1.8$$

Where λ is wavelength of the emission in nanometer, T is absolute temperature in K Substituting T = 310 K (37 °C normal human body temperature) in equation 1.3 yields a value for λ of 9348 nm or approximately 10 µm. In fact, radiation from the human body is considered to lie in the range of 8-14 µm, hence infrared sensors that are sensitive in this range would be able to detect humans within their detection area, (<http://hyperphysics.phy-astr.gsu.edu> accessed on 23rd October 2021).

1.3 Statement of the problem

Gas leakages, fire outbreaks and human intrusion are some of the problems faced in our homes and industries. Several advancements to solve these security problems have been identified. Among the advancements is the use of MQ-4 gas sensor in gas leakage. The sensor has been developed and tested under ideal conditions of its sensitivity. However, different environments correlate differently on its sensitivity. The output sensitivity of the MQ-4 gas sensor depends on the conductivity which in turn depends on environment and correlate with ideal characterization. Therefore, the need to investigate its characterization in real environment is key for optimum output. This research will investigate the characterization of MQ-4 gas sensor in real environment in relation to ideal sensitivity characterization. Intrusion to offices, homes and industries is a great menace in our today world. PIR has played a key role in security advancement, but further investigation on characterization of PIR sensor aimed at assessing the impact of three factors; proximity, placement point of the PIR sensor for high recognition rate and the sensors sensitivity are key. Fire outbreaks have been a great threat to both lives and infrastructures hence, its prevention is paramount. The sensors over time have been developed, but environmental factors especially air-mass has made them to fail severally. The need to characterize the sensor depending on environment is key in realisation of optimum results. The interfacing of these key sensors through a microcontroller is key for the optimization of the home security system.

1.4 Justification

This research seeks to develop an integrated microcontroller based home security system to detect intruders, fire outbreaks and gas leakage. The characterization of the MQ-4 gas sensor will allow the sensor to adapt to different environments since its sensitivity depends on the conductivity which in turn depends on environment. The characterization of PIR sensor aimed at assessing the impact of three factors; proximity, placement point of the PIR sensor for high recognition rate and the sensors sensitivity are key. This will allow the system to optimize on intruder detection. The success of the research will build

a platform for upgrading the conventional security system to automated system that will require little of human intervention. Additionally, it will provide a cost effective and more efficient security system in areas such as homes as well as industries.

1.5 Research hypothesis

There is no optimization of the sensors in the security enhancement from the developed integrated microcontroller based home security system.

1.6 Research objectives

1.6.1 General objective

The characterization and optimization of MQ-4 gas sensor, PIR sensor and temperature sensor in an integrated microcontroller based home detection security system.

1.6.2 Specific Objectives

1. To characterize the MQ-4 gas sensor using standard prepared alcohol fluid and correlation with ideal sensitivity characteristics of MQ-4 gas sensor.
2. To characterize the PIR sensor through the measurement of absorption of IR radiation at different spatial positions and speeds in correlation with their outputs in PIR sensor.
3. To optimize temperature sensor at different voltage levels.
4. To integrate the characterized and optimized sensors with a microcontroller and output devices and test its performance

CHAPTER TWO

MATERIALS AND METHODS

2.1 Introduction

This chapter discusses the instruments and procedures used in the design and calibration of the MQ-4 gas sensor, the infrared sensor, the temperature sensor and integration of these modules into a microcontroller based home security system.

An experimental set-up was designed in the laboratory. Data using the sensors was captured and recorded. A programmed code was formulated for the integration of the three sensors. Data recorded was analyzed and results presented.

2.2 Design methodology

The block diagram of Figure 2.1 shows the various modules which were integrated to form the proposed home security system.

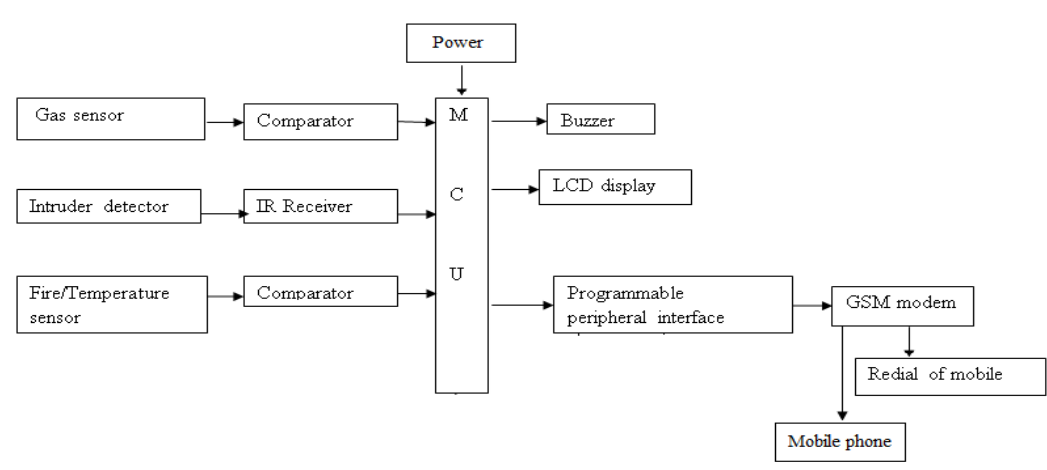


Figure 2.1: Block diagram of modules and their interconnection

The system is composed of gas, fire/temperature and intrusion sensors. The gas sensor detected any gas leakage and produced a signal which was fed to the comparator which compared the gas concentration with a predetermined value. The signal strength was dependent on the concentration of the leaked gas. If the signal was above the optimum value for the sensor, the buzzer went on and the owner was alerted. The gas concentration was then displayed on an LCD display. Simultaneously an SMS was sent to a configured SIM card for mobile alert.

The intruder sensor consisted of an IR source and two IR detector slots separated by a distance in which the infrared rays from source were equally received. If any of the IR rays directed from the slots was obstructed, the negative differential of IR intensity was fed to the microcontroller as a signal. This signal was fed to the outputs which alerted the owner through switch ON of buzzer, display on LCD and sending of short message.

The fire sensor detects any possible fire outbreak in the house. This is done by use of piezoelectric disc. Once the predetermined value of the temperature was reached, a signal code was fed into the microcontroller and an alert was sent to the outputs. The LCD displayed 'FIRE' and the buzzer went ON. A short message was sent to the configured SIM card to alert the home owner.

The sensors experimental processes were set up and observations made over time. The performance parameters for each sensor were put into consideration as discussed in the methodology part. Results obtained were tabulated, analyzed and graphs drawn for interpretation in chapter three.

2.3 The hardware design modules of the proposed microcontroller security system.

This section discusses modules shown in the Figure 2.1 in more details.

2.3.1 Gas sensor module

The gas sensor used was MQ-4 semiconductor sensor for cooking gas. Tin (IV) oxide (SnO_2) is the sensitive material of MQ-4 gas sensor which has a low conductivity in clean air. When a target combustible gas exists, the sensor's conductivity increases as the gas concentration rises. Figure 2.2 shows a schematic diagram of the set up for testing the MQ-4 gas sensor.

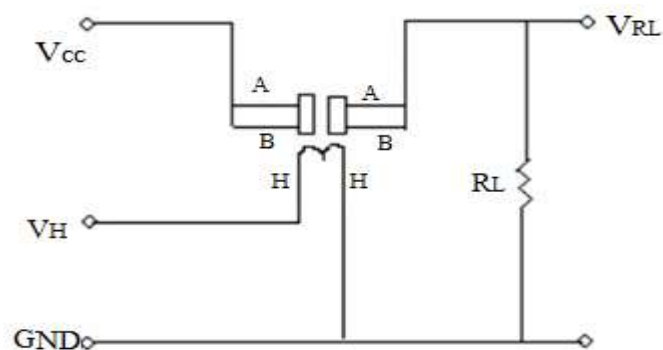


Figure 2.2: A schematic test circuit of MQ-4 gas sensor

The heating voltage V_H , supplies working temperature to the sensor, while V_{CC} is the source voltage and V_{RL} is voltage drop across load resistance (R_L). Internal resistance A-B between points A and B of the gas sensor, varies with the concentration of the target cooking gas. Point H-H represents the heating filament. The circuit can be simplified as shown in Figure 2.3, where R_s is the MQ-4 gas sensor internal resistance. The pin to Arduino sensor is used to get digital output from this pin, by setting a threshold value.

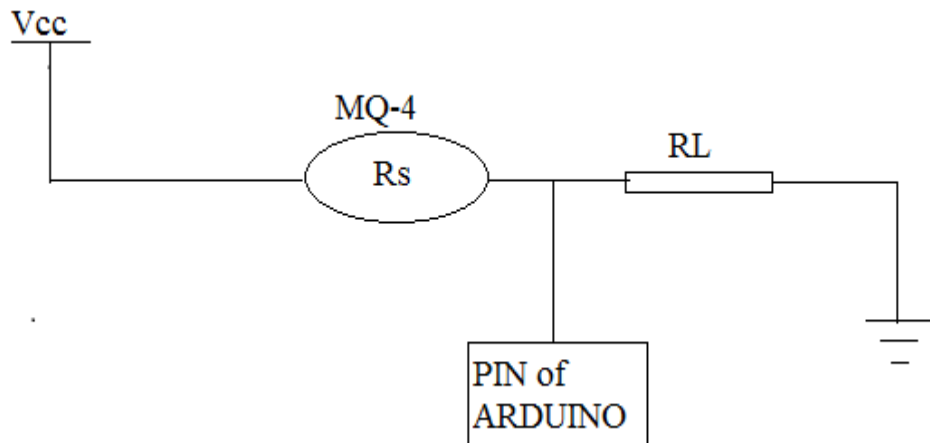


Figure 2.3: Simplified circuit of MQ-4 gas sensor. RL and Rs resistors are connected in series.

Table 2.1 shows the datasheet of sensitivity characteristics of the MQ-4 gas sensor from which the information was utilized in pre heating of the MQ-4 gas sensor.

Table 2.1: Datasheet of sensitivity characteristics of MQ-4 gas sensor (www.hwsensor.com).

Symbol	Parameter name	Technical parameter	Remark 2
R_s	Sensing Resistance	10K Ω - 60K Ω (1000ppm CH ₄)	Detecting concentration scope: 200-10000ppm CH ₄ , natural gas
α (1000ppm/ 5000ppm CH ₄)	Concentration slope rate	≤ 0.6	
Standard detecting condition	Temp: 20°C \pm 2°C Humidity: 65% \pm 5%	Vc: 5V \pm 0.1 Vh: 5V \pm 0.1	
Preheat time	Over 24 hour		

2.3.2 Design and instrumentation of simulation circuit of the MQ-4 gas sensor module.

Figure 2.4 shows the schematic diagram of the circuit topology designed and simulated in electronic work bench software. The circuit consists of a battery (5V) which is the voltage source of the circuit, resistor (R_1) which represents the internal resistance of the MQ-4 gas sensor and the variable resistor (R_2) connected in series with R_1 . This procedure was necessary in order to investigate the optimum resistance, R_L of the design and establish their working values. The voltage drop across R_L was measured at different resistances and displayed on a digital display as shown in Figure 2.4. The virtual circuit was thereafter tested by mounting it on a solder-less breadboard and the real data collected for comparison with the synthetic data.

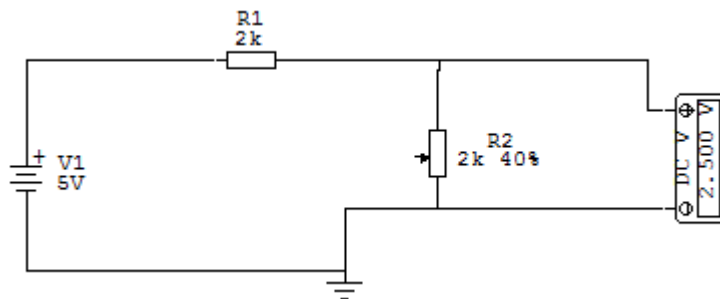


Figure 2.4: Simulation circuit of finding optimum resistance

2.3.3 Heating of MQ-4 gas sensor for sensitivity adjustment

The resistance value of MQ-4 is different for various kinds and concentrations of gases (Hanwei Electronics). So, when using this components, sensitivity adjustment was very necessary. The manufacturer recommends the calibration of the detector for 5000 ppm of CH_4 concentration in air and value of load resistance (R_L) about 20 K Ω (10 K Ω to 47 K Ω) be used. When accurately measuring, the proper alarm point for the gas detector should be determined after considering the temperature and humidity influence.

The MQ-4 gas sensor hence needed heat-up time before the first usage. The enveloped MQ-4 has 6 pins, four of them are used to fetch signals, and other 2 are used for providing heating current. The two central pins of the MQ-4 gas sensor were used to provide the heating current.



Plate 2.1: Diagram showing how MQ-4 was heated up.

2.3.4 Preparation of methanol solution

Eleven different methanol solutions of concentrations (ppm) 500, 1000, 2000, 3000, 4000, 5000, 6000, 7000, 8000, 9000 and 10000 were prepared through the procedure as outlined by Tinas (2008). Volumes of 99.8% concentrated methanol were measured using graduated pipette fitted with rubber pipette filler and solutions prepared using de-ionized water. The measured concentrated methanol was added to a 250 ml volumetric flask which contained de-ionized water. The mixture was stirred for 5 minutes so as to ensure formation of homogenous solution. The solution was then topped up with de-ionized water up to the mark. The concentration is a measure of the volume of methanol in 1000 ml/l of the aqueous solution with de-ionized water. In this case, de-ionized water is considered 0% concentration. The proportion of methanol in 1000 ml of the solution is

taken as the parts per million concentrations. The volume of methanol to be added to make the required concentrations was deduced through several steps. The density, mass and volume calculation can be done in the following way:

$$M = \rho \times V \dots\dots\dots 2.1$$

Where M is mass, ρ is density and V is volume. Equation 2.1 is working in case of a pure fluid. As in this case a 99.8% methanol is chosen hence we add the factor of concentration in our equation 2.1.

$$M = \rho \times V \times C \dots\dots\dots 2.2$$

Where M is mass of alcohol in standard concentration fluid ρ is density of pure methanol, V is volume of methanol and C is concentration of methanol. After reformulating equation 2.2, the value of V can be found:

$$V = \frac{M}{C \times \rho} \dots\dots\dots 2.3$$

In this step, 1 liter 10000 PPM standard concentration of methanol fluid is mixed. According to equation 2.1, the purpose is to get 1 liter 10000 PPM standard fluid and 10000 PPM equal to 10000 mg/l. Therefore; there is 10000 mg pure methanol in the fluid. The mixing process will consider the mass of pure methanol, the density of methanol at 20 degrees Celsius and the concentration of methanol fluid. Using equation 2.3 V equals to 12.6 ml. So, 12.6 ml of methanol was mixed with de-ionized water until the whole volume was 1 liter. Now, there is a 1 liter 10000 PPM standard concentration of methanol fluid mixed. This fluid includes 10000 mg pure alcohol and it follows that 10000 PPM equal to 10000 mg/l.

2.2.5 Experimental set up for gas sensor module

The diagram below shows the flow chart of the MQ-4 sensor sensitivity adjustment process.

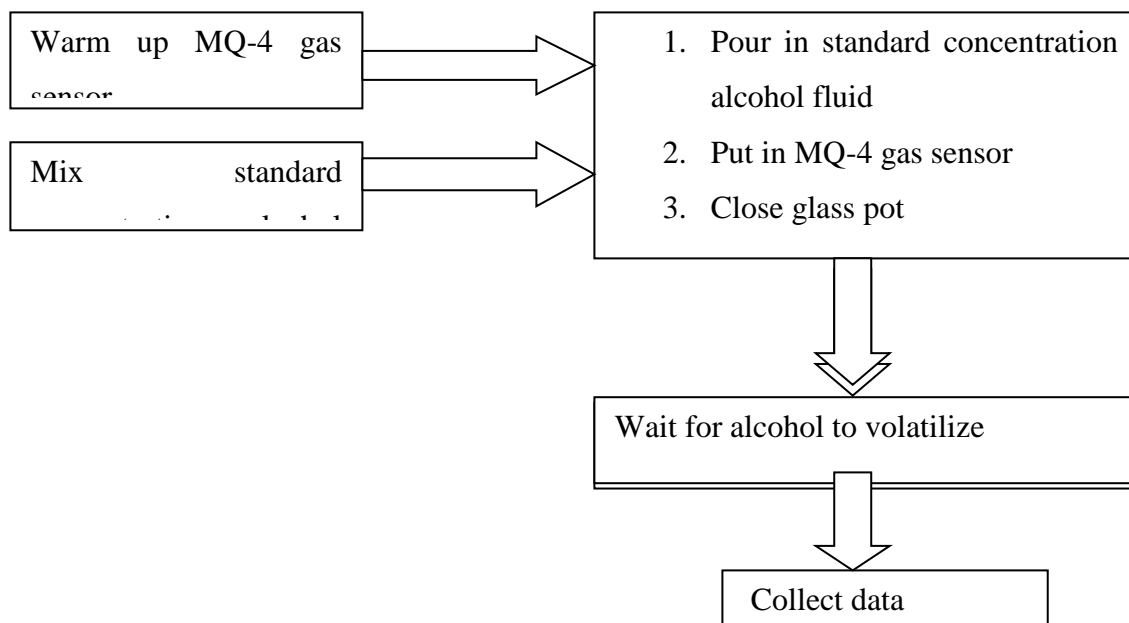


Figure 2.5: Flowchart diagram of the MQ-4 sensor sensitivity adjustment process

An almost closed glass pot was used to create a closed and stable measurement environment. An aluminum foil was used to totally cover the open of the glass pot. The glass pot had a volume of 250 ml so as to provide space for the gas sensor and the connecting wires of the circuit. Knowing the latent heat of vaporization of methanol at 25°C to be 37.43 kJmol⁻¹, the normal room temperature could vaporize the methanol solution. The ideal data sheet is as shown in figure 2.6 below.

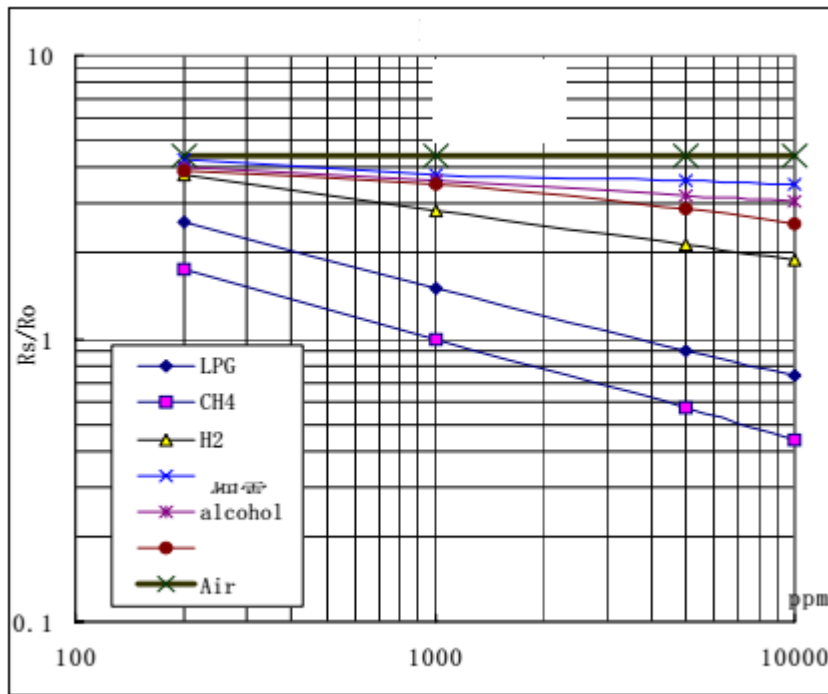


Figure 2.6: Ideal sensitivity characteristics of MQ-4 gas sensor (Pololu robotics and electronics)

2.3 Infrared Sensor module

2.3.1 Introduction

The electromagnetic spectrum contains infrared radiation, which has a wavelength longer than visible light and cannot be seen but may be sensed. Animals and the human body, whose infrared radiation is highest at a wavelength of 9.4 μ m, are among the objects that produce heat and infrared radiation. Motion can be detected using passive infrared sensors (PIR), which are also used to determine whether an obstruction has moved into or out of the sensor's field of view.

2.3.2 The PIR Sensor

The PIR sensor's internal design is depicted in Figure 2.7. The extremely high impedance of the sensors is buffered by a junction gate field-effect transistor (JFET), which has a very low noise floor. To increase its tolerance to noise, temperature and humidity, the infrared radiation (IR) sensor utilized in this project is placed in a hermetically sealed metal container. The sensor element is shielded by a window formed of IR-transmissive material, which is generally coated silicon because it is relatively accessible. The two balancing sensors are located behind the window.

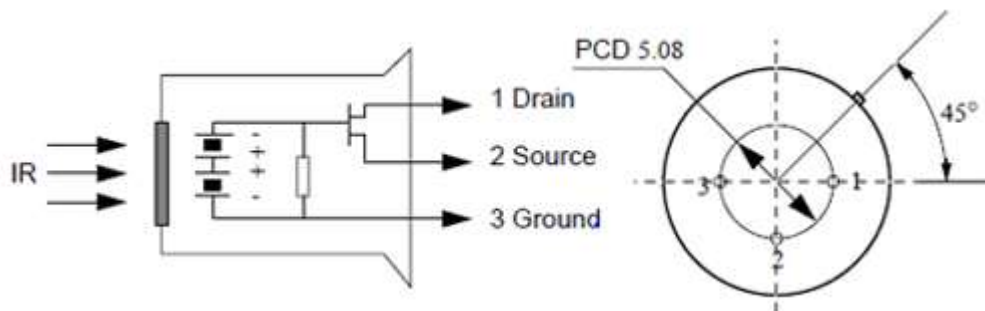


Figure 2.7: Internal schematic diagram of passive infrared sensor.

2.3.3 How PIR Work

A pyroelectric sensor is the PIR. A pyroelectric sensor is constructed of a crystalline substance that, when subjected to heat in the form of infrared radiation (IR), produces a surface electric charge. A sensitive FET device that is incorporated into the sensor can monitor the change in charge when the amount of radiation striking the crystal varies. According to Figure 2.8, the PIR sensor consists of two slots, A and B. An IR-sensitive fused silica is used to make each slot. When the sensor is not in use, both slots will detect the same quantity of IR, which is equal to the amount of radiation being emitted outdoors. When environmental factors like temperature fluctuations and sunshine

concurrently affect both elements and cause them to create the same amount of output but with opposing polarities, they will cancel each other out. When one of the sensor's elements is exposed to a change in radiation while the other is at rest, the output voltage of the sensor changes. The intruder's path is shown by the arrows A and B.

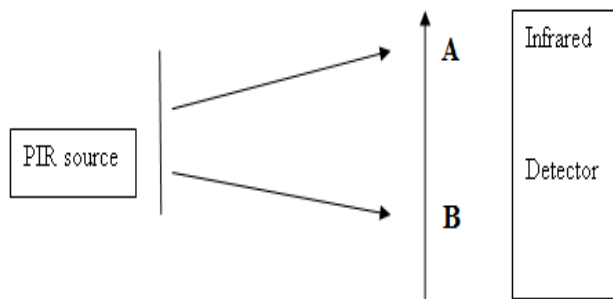


Figure 2.8: Schematic diagram illustrating PIR functioning

A positive differential shift between the two slots is recognized as a signal and recorded as soon as the move of a heated body is observed. The sensor will produce a negative differential change that can be observed once the heated body has left the sensing area. What is detected are these change pulses.

2.3.4 Detecting area coverage

The lens may quickly and simply alter the width, range, and sensing pattern. The infrared light can trigger a signal in the sensor because of the substantially bigger detecting area. Without a lens in front of the sensor, if an IR emitting body moves across the sensor's front at a distance of 3 to 4 feet from the sensor, the radiated IR will expose one element more than the other, producing a voltage output. There is no voltage output, however, when the IR emitting body is farther from the sensor and its radiation pattern blurs, exposing both elements more equally. The detection range of the sensor is increased by placing a lens in front of it. The infrared light can trigger a signal in the sensor because of the substantially bigger detecting area when an IR emitting body rather than a lens is placed in front of a sensor. The sensors are actually Fresnel lenses as

a result. The Fresnel lens concentrates light, giving the sensor access to a wider range of infrared radiation. Utilizing the materials at hand is essential to the project; one example is the comparison of sensitivity and area coverage using basic lenses like those used in cameras.

2.3.5 PIR sensor characteristics for objects at different distances and heights

The purpose of this study was to evaluate the effects of three variables on the proximity and placement point of the PIR sensor for high recognition rate and sensor sensitivity, namely the height of sensor location, the vertical distance between the PIR node, and movement of the human body, including (i) across the detection area at different distances for different walking speeds, (ii) walking towards the detector, and (iii) walking away from the detector at different angles. The space is 7 m by 7 m in size. The heights of the sensors are 0.5, 1.0, 1.5, and 1.8 m. The portions of the human knee, hand swing, chest, and head are represented by heights of 0.5, 1.0, 1.5, and 1.8 m, respectively. The test objects were asked to walk along the established six lines indicated as 1,2,3,4 and 5 at various speeds. The heights of various human bodies are shown in Table 2.2.

Table 2.2: Attribute Features of Experiment Object

Object	Height (m)	Step distance. (m)
A	1.70	0.50
B	1.74	0.52
C	1.69	0.50
D	1.64	0.41
E	1.60	0.37

The output from all the items is captured when the subject passes over each arc or radial line of the PIR detector. The detector's five analog signals are detected, and each signal is given equal weight. Using equation 3.1, the results taken into consideration for the analysis are computed.

$$X_i = X_1 + X_2 + X_3 + X_4 + X_5 \dots \dots \dots 2.7$$

Where the raw output voltages for objects A, B, C, D, and E are X1, X2, X3, X4, and X5. Equation 3.2 is used to determine the root mean square value of a detector output voltage over an arc or radial line.

$$V_i = \sqrt{\frac{\sum_{i=1}^n X_i^2}{n}} \dots \dots \dots 2.8$$

Where X_i is the detector output from equation 3.1 over an arc / radial line; and N is the number of detector data points on a given arc/radial line.

2.4 Temperature measurement with LM35 temperature sensor

Without requiring a lot of operator input, the temperature in the kitchen was monitored and managed using the LM35 integrated circuit (IC) sensor. With an electrical output proportional to the temperature (in °C), the LM35 is an integrated circuit sensor that may be used to measure temperature.

2.4.1 LM35 Temperature Sensor

Precision integrated-circuit (IC) temperature sensors of the LM35 series have an output voltage that is linearly proportional to the temperature in Celsius (Centigrade). Thus, compared to linear temperature sensors calibrated in Kelvin, the LM35 has an advantage because the user does not need to deduct a significant constant voltage from its output to obtain suitable Centigrade scaling. The LM35 can give typical accuracies of 0.25°C at room temperature and 0.75°C over the entire temperature range of 55 to +150°C without the need for any external calibration or trimming. Trimming and calibration at the wafer level ensure low cost. It is particularly simple to interface to reading or control circuitry thanks to the LM35's low output impedance, linear output, and excellent intrinsic calibration. It can be used with a positive or a single power source. Both a single power

supply and positive and negative power supplies can be utilized with it. It only draws 60 A from its supply, therefore it self-heats very slowly—less than 0.1 C in calm air. The operating temperature range for the LM35 is 55 to 150 C, whereas that for the LM35C is 40 to 110 C. Hermetic TO-46 transistor packages are available for the LM35 family. Figure 2.9 displays the LM35 IC's schematic diagram. The positive voltage supply pin, known as +Vs, ranges in voltage from 4 to 20 volts. The analog output pin for the temperature sensor is labelled OUTPUT. Its temperature range is between +2 ° C to 150 ° C

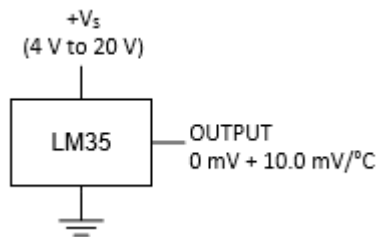


Figure 2.9: Basic Centigrade Temperature Sensors

2.4.2 ADC0831 Analogue-to-digital Converter

An analogue to digital converter (ADC) is needed since the LM35's output is an analog voltage that must be transformed into a digital signal before the microcontroller can process it. For this procedure, an ADC 0831 analogue to digital converter will be employed. Figure 2.10 displays the ADC 0831 IC's schematic diagram.

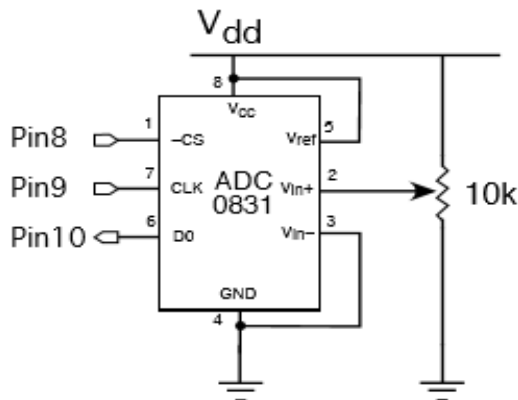


Figure 2.10: A schematic diagram of the ADC0831 ADC

The ADC0831's inputs and outputs are represented by the following notation: $V_{in} (+)$ serves as the analog input, while $V_{in} (-)$ and V_{ref} are utilized to bias the IC. $D0$ serves as the serial output. For powering the IC, V_{cc} and GND are used. GND equates to V_{ss} , while V_{cc} is nearly the same as V_{dd} . Active low chip select (CS) and clock (CLK) are the respective abbreviations. For binary control signals, both serve as inputs. The $-CS$ pin needs to receive a signal that starts high and goes low from the BASIC Stamp in order to prime the ADC0831 for taking a measurement. Throughout the conversion, this signal must remain low. The conversion should then begin at the subsequent clock pulse, which must be indicated by sending one clock to the CLK input. A clock pulse for this IC begins low, rises to a high, and then falls back to low. The conversion requires eight more clock pulses to be completed. The CLK input receives a clock pulse, while the $D0$ output sends another serial bit each time.

2.4.3 Process of Measurement with LM35 Temperature Sensor

The analogue digital converter's (ADC) primary use is to digitize a temperature sensor's output. The LM35 is a simple-to-use temperature sensor. The LM35 produces a voltage that is temperature-related. The most popular model of this measures temperatures between 0 and 100°C by providing an output voltage equal to 10 mV times the temperature in degrees Celsius. Therefore, 20 °C would result in 20 mV.

The device has three terminals i.e. 5V, ground and output as shown in the diagram of Figure 2.11.

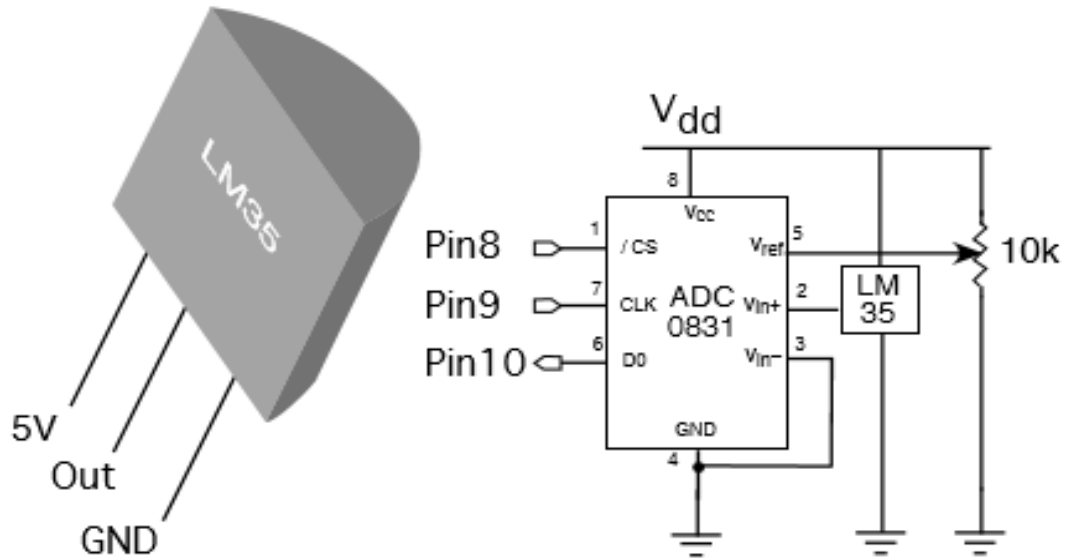


Figure 2.11: (a) Pin out diagram of LM35 temperature sensor (b): Schematic diagram of LM35 temperature sensor connected to ADC0831 converter

The output acts like a voltage source whose voltage is proportional to temperature in degrees Celsius, i.e.

$$V_{out} = (10 \text{ mV}/^{\circ}\text{C}) T \dots\dots\dots 2.9$$

To connect a potentiometer to an ADC converter and adjust the upper limit of the ADC range, see Figure 2.10 (b). A display subroutine is created to print out the temperature in degrees Celsius while V_{ref} is set to be 0.51 V.

A little device that collects data and stores it for later retrieval can be useful at times. The stamp may be quickly converted into a temperature logger that can be installed somewhere to record temperatures at regular intervals. Other than its 9V battery, the micro-controller doesn't require connection to any other computer or power source.

The data can then be downloaded onto another computer for analysis and long-term storage when it is later brought back to the lab. The WRITE instruction is used in the program below to store data permanently in EEPROM. For 1000 s (16.7 min), it records temperatures every 10 s, and then it quits. The data must be obtained using a different software, although downloading the retrieval program does not affect the recorded data.

2.5 Arduino Uno Microcontroller

The processor (the CPU), non-volatile memory for the program (ROM or flash), volatile memory for input and output (RAM), a clock, and an input/output (I/O) control unit are all found on a single chip in a microcontroller. A general block diagram of an Arduino microcontroller is displayed in Figure 2.12. Before transferring the information to the output devices, it receives the data or information from various sensors and compares it with the relevant predefined limits.

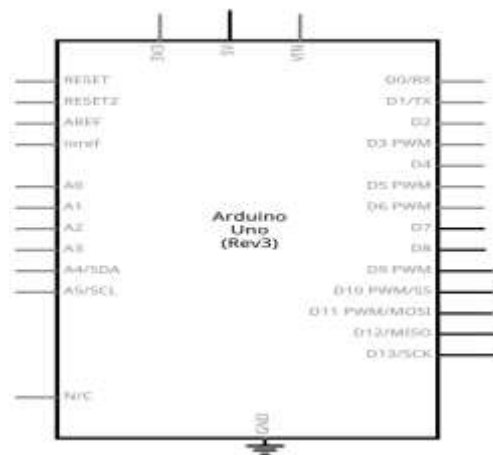


Figure 2.12: Pin diagram of Arduino Uno (Rev3) microcontroller

A serial channel can be used by an Arduino to send or receive data. The Arduino can communicate with any device that is capable of serial communication. Whatever

programming language is powering the other device is irrelevant. The "main" serial port on the Arduino can be used, or one can reserve that channel for programming (and the serial monitor in the development environment) and utilize two other pins for a second serial link just for the external device. Some applications lack native serial capabilities, such as Flash. They can still communicate with Arduino by using a middleman who acts as a sort of "translator" and lets them speak to one another.

The on-board LED may be turned ON or OFF using an external switch and the Arduino board. When the push button is not depressed, a switch coupled with a resistor ensures that the Arduino's digital input pin 7 is always linked to a steady voltage of +5V. The signal on pin 7 goes to ground (GND) when the push button is pressed. The Arduino's +5V supply is simultaneously connected to GND, and a current resistor of 1 to 10 K is employed to prevent short circuits. The input pin would act as though it were "floating" anytime the pushbutton was not depressed if there was absolutely no connection between pin 7 and +5V. This indicates that it is not connected to either GND or +5V, allowing electrostatic noise to collect and cause an input to falsely trigger. The gas, intrusion, and temperature sensors send analogue voltage signals to the Arduino Uno microcontroller. After converting to digital signals, it determines if the received values are within the microcontroller's predetermined range. If the signals fall within the predetermined ranges, no alerts are sent to the owner; however, if they rise above the predetermined ranges, signals are sent to the buzzer, LCD display, and authorized GSM module.

The Arduino Uno microcontroller receives the analogue voltage signals coming from the gas, intruder and temperature sensors. After conversion into digital signals, it checks where the values received are within the set values for the microcontroller.

If the signals are within the set values the outputs do not alert the owner, but if they are above the set ranges then it sends signals to the buzzer, LCD display and to the authorized GSM module.

2.6 LCD display

In order to display the data from the microcontroller, a liquid crystal display (LCD) is used. Results from the gas sensor, intrusion detector, and fire/temperature sensor are displayed on the 16*2 LCD monitor, which is part of the system.

2.7 Buzzer

When the sensor temperature reaches 40 °C or higher, when gas detection exceeds 697.01678 mV ppm, or when an intruder is discovered inside the sensor's detection range, a buzzer is utilized to produce a sound. This buzzer was selected since it is affordable, dependable, and easily accessible.

2.8 Programmable peripheral interface

It is utilized for interfacing and connecting peripheral devices. Input-output device is another name for the peripheral device. Input and output devices are connected to computers using the input and output ports.

2.9 GSM modem.

Short message transmission (SMS) over a GSM module is required to deliver this information to the home owner or authorized agent in the event of a fire, intruder, or gas leak detection.

This is accomplished by connecting a PPI to the Arduino microcontroller through a GSM module that has been set up to receive such a message.

2.10 System circuit diagram of the Hardware design

The Figure 2.13 shows all connections of sensors and outputs to the Arduino Uno microcontroller to implement the proposed microcontroller based home security system. The 5V is supply voltage pin. The GND is ground pin. So, the gas sensor, temperature

sensor, and intruder sensor supply voltage, were provided by 5V. And all these three devices should be connected to GND to consist a complete circuit.

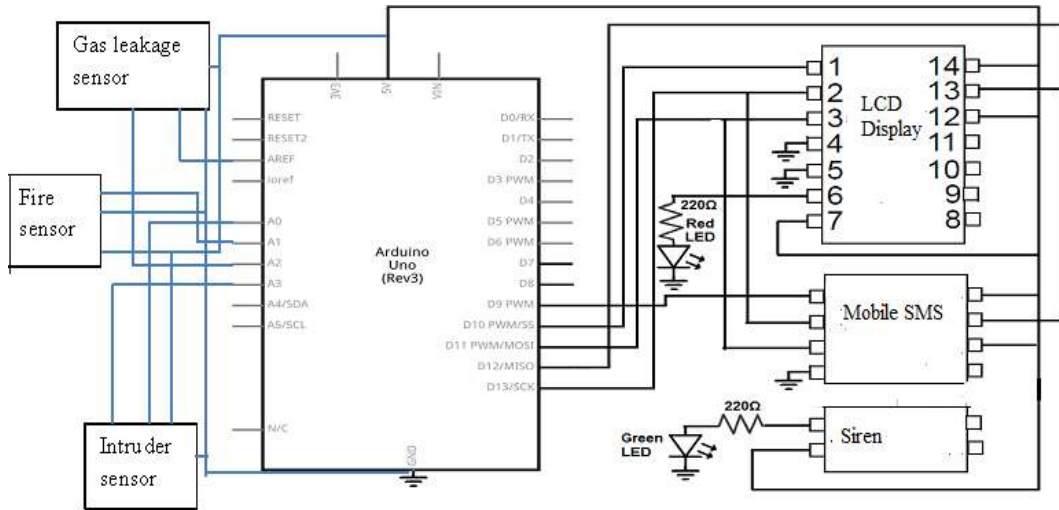


Figure 2.13: Circuit diagram of the Arduino Uno based security system

Figure 2.14 flowchart shows how the sensors operate. The signal is transferred to the programmable peripheral interface for comparison processing before being handed on to the output devices by the MQ-4 gas sensor when it detects gas leakage and the threshold point has been exceeded. The PIR detector and the fire/temperature sensor follow the same pattern. The security system is said to be in a "idle" condition when there is no detection. Figure 2.13: Circuit diagram of the Arduino Uno based security system.

2.11 System circuit diagram of the Software design

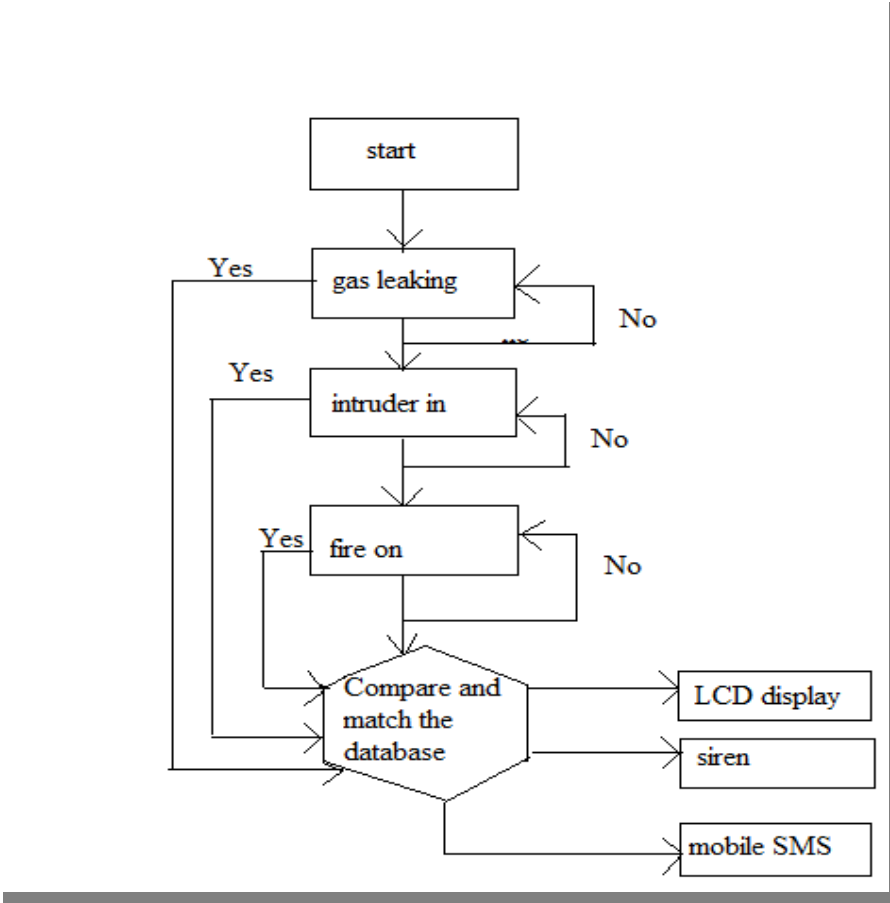


Figure 2.14: Flowchart depicting functioning of the security system

CHAPTER THREE

RESULTS AND DISCUSSION

3.1 Introduction

This chapter presents and discusses the results of the data collected about the gas, PIR and temperature sensors. According to the methodology information in the chapter 2, the collected data has been presented in graphical forms. The sensors are then integrated with the microcontroller to form the integrated security system.

3.2 Analysis of MQ-4 Gas Sensor in Ideal Situation

Figure 2.4 shows a simplified circuit of calibrating the MQ-4 gas sensor as given by the manufacturer and has been described in methodology in Chapter 2.

The formula of the sensing resistance R_s , of the gas sensor is deduced from the data sheet of MQ-4 gas sensor as:

$$R_s = \left(\frac{V_{CC}}{V_{RL}} - 1 \right) \times R_L \dots\dots\dots 3.1$$

Resistor R_L was carefully chosen using the data sheet to optimize the output results. The value of R_L was found to be 2.0 k Ω . According to Figure 2.6, methanol was used to substitute for methane, since their sensitivity characteristics are similar. R_s is the sensing resistance of the gas sensor and it has a range depending on the type of the gas and concentration. From the Figure 2.6 the ratio of R_s/R_o was found to be 4.5 in air. In order to get the R_s value, R_o was calculated in advance. The output voltage (V_{RL}) was measured in clean air and was equal to 0.6 V. Supply voltage (V_{CC}) was measured to be 5.1V. Then according to equation 3.3, R_s was calculated to be 15 k Ω in clean air. Since $R_s/R_o = 4.5$ in clean air, R_o becomes 3.33 k Ω . Because the value of R_o is constant values of R_s are given in Figure 2.6 for different concentration. Finally, the output

voltage of the gas sensor, V_{RL} , was calculated using equation. 2.6. From the ideal characteristics, the ratio of R_s/R_o of the alcohol were obtained and used in calculation of R_s using equation 3.3. From Figure 2.3, R_L resistor and R_S resistor are in a series circuit. R_o is a constant of $3.33\text{ k}\Omega$ as calculated in equation 3.3. Figure 2.6 shows the ideal characteristics of the MQ-4 gas sensor as provided by the manufacturer. This is before the MQ-4 is exposed to the methanol at different concentration in parts per million.

The data of the MQ-4 gas sensor from the manufacturer is plotted in Figure 3.1 as a graph of output voltage against the concentration in ideal conditions.

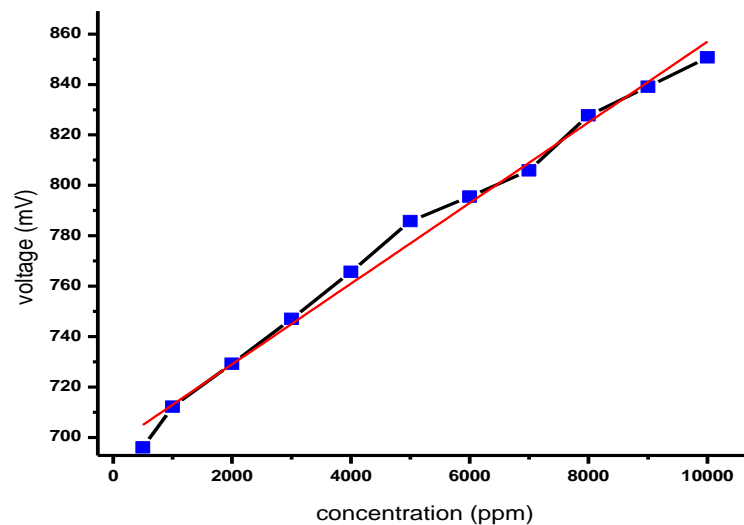


Figure 3.1: A graph of voltage, V_{RL} (mV) versus concentration (ppm) of methanol for the MQ-4 gas sensor for methanol under ideal conditions.

The line of the best fit of Figure 3.1 is given by the equation $y=0.01599x+697.02$. From the equation it follows that the MQ-4 gas sensor registered a voltage of 697 mV when it was not exposed to alcohol.

3.2 Calibration of the MQ-4 gas sensor using methanol.

The plate below shows how the calibration of MQ-4 gas sensor was done. The methanol gas which has similar characteristics as the LPG gas was used to collect the data.

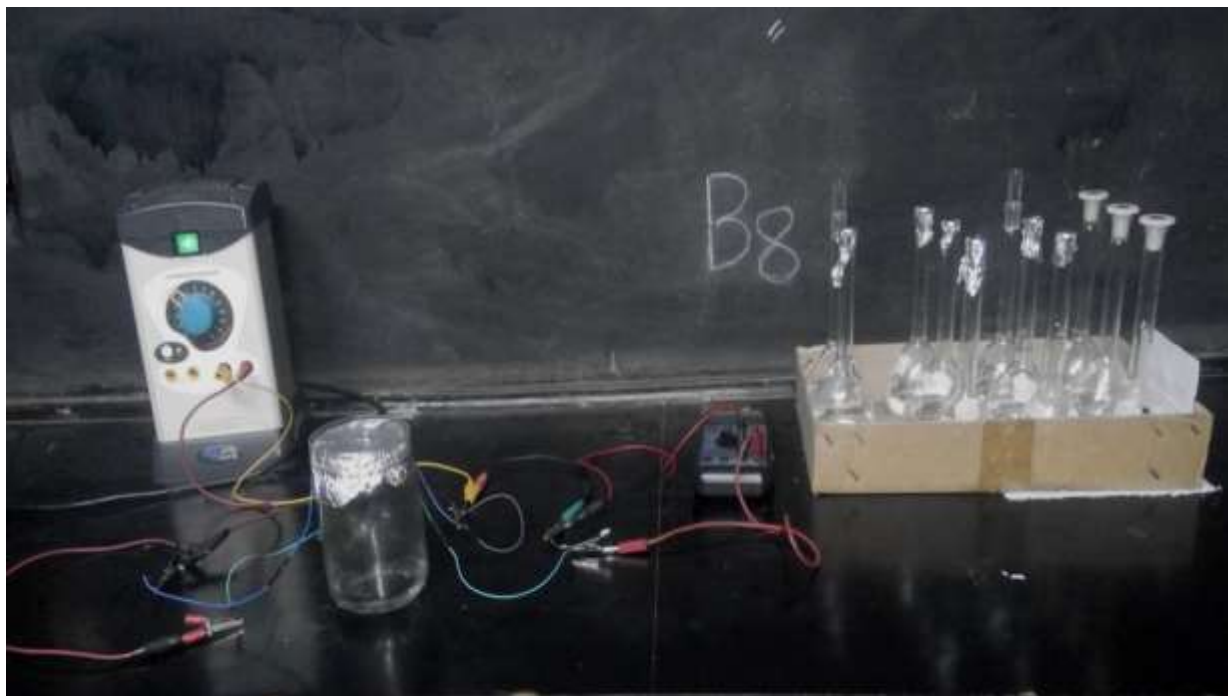


Plate 3.1: The experimental arrangement set up to measure voltage drop across resistor R_L when the MQ-4 gas sensor is exposed to different concentrations of methanol.

Figures 3.4 to 3.8 show the results for voltage of the MQ-4 gas sensor for one, two, three, four and five days of pre-heating. In each figure the data is compared with the theoretical value. The pre-heated MQ-4 gas sensor is exposed to methanol for five, fifteen, thirty, and forty-five minutes and voltage recorded respectively.

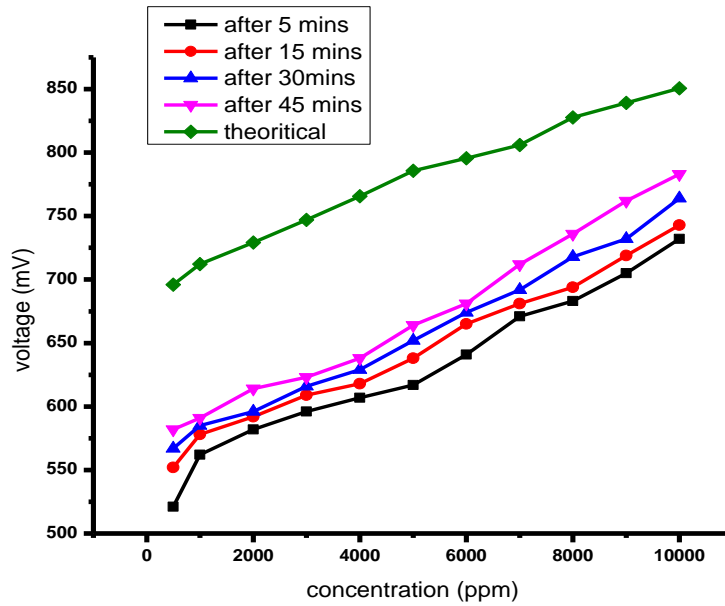


Figure 3.2: Graph of output voltage (mV) versus concentration of methanol (ppm) in different exposure-time after 24 hours of heating MQ-4 gas sensor.

From the graph profile the theoretical and experimental values differ so much hence the optimum value could not be obtained after one day of pre- heating. After two days of the pre-heating the MQ-4 sensor the results are plotted in Figure 3.3 were obtained. The results shown is after the sensor was exposed to methanol gas for five, fifteen, thirty and forty-five minutes respectively.

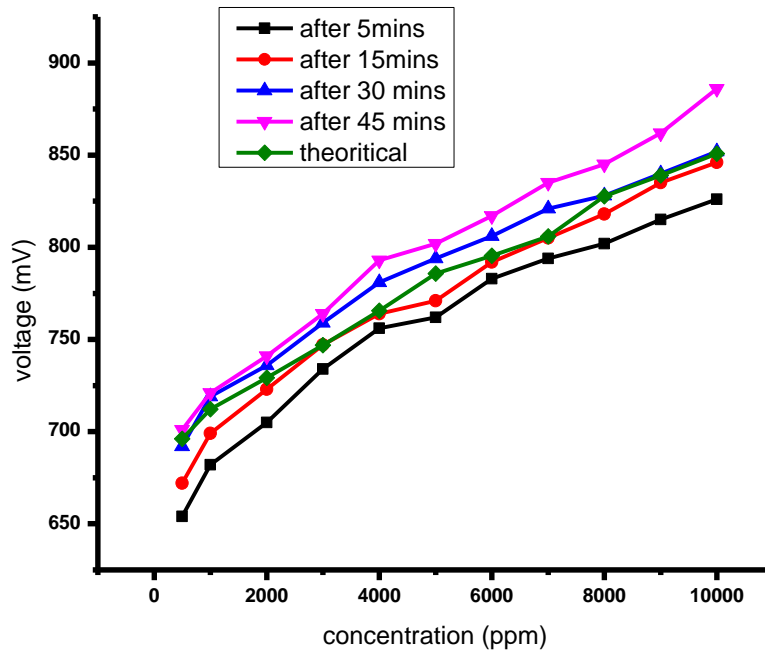


Figure 3.3: Graph of output voltage (mV) versus concentration of methanol (ppm) in different exposure-times after 2 days of heating MQ-4 gas sensor.

From Figure 3.3 the graph the theoretical values and experimental values obtained after 2 days pre-heating of MQ-4 gas sensor were very close. The exposure time between 15-30 minutes gave a close tally to our ideal conditions hence a high agreement between the theoretical value and experimental value.

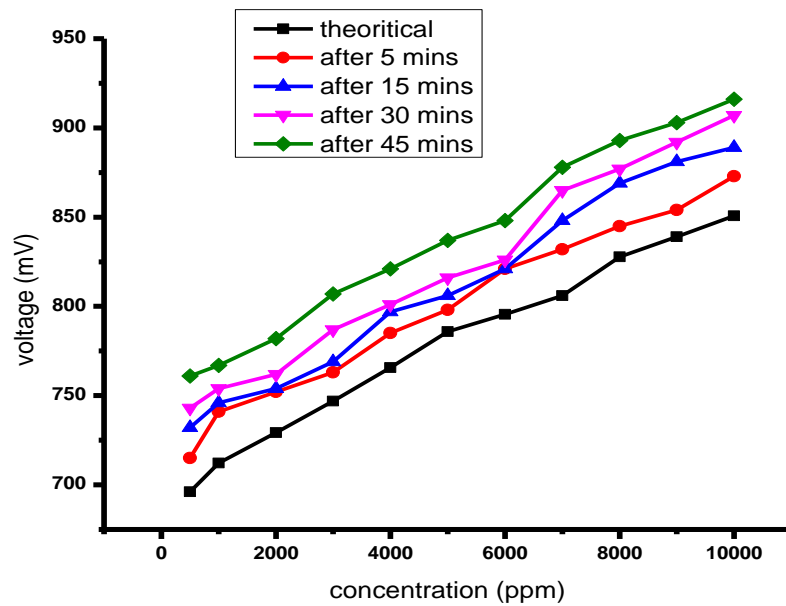


Figure 3.4: Graph of output voltage (mV) versus concentration of methanol (ppm) in different exposure-times after 3 days of heating MQ-4 gas sensor.

A graph of voltage (mV) versus concentration of methanol (ppm) three days in different heat-time. Figure 3.4 shows some deviation between the ideal conditions and the real conditions. This may be attributed to a long pre-heating time of the MQ-4 gas sensor.

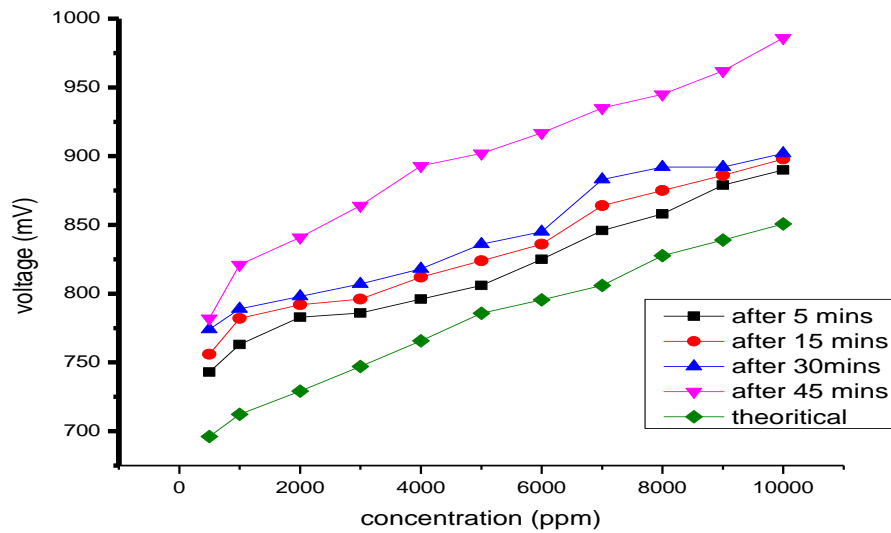


Figure 3.5: Graph of output voltage (mV) versus concentration of methanol (ppm) in different exposure-times after 4 days of heating MQ-4 gas sensor.

The results from Figure 3.5 shows a deviation of the theoretical results from the real results. This may be attributed to more pre-heat up time of the MQ-4 gas sensor hence not giving more optimum temperature.

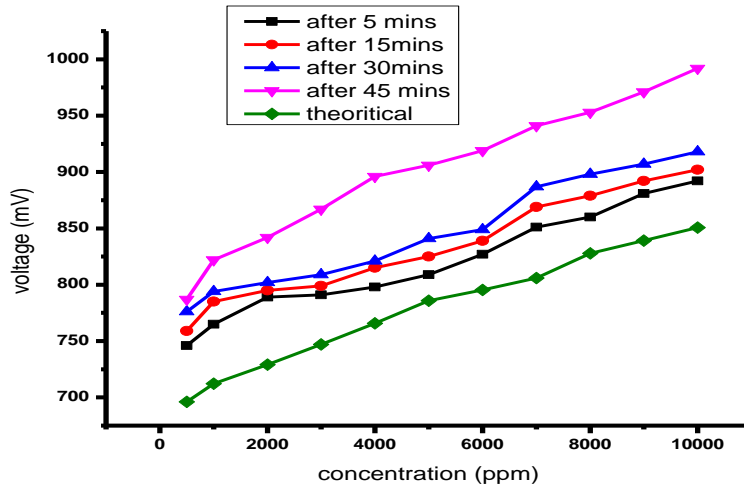


Figure 3.6: Graph of output voltage (mV) versus concentration of methanol (ppm) in different exposure-times after 5 days of heating MQ-4 gas sensor.

Generally, the output voltage is almost stable after two days of pre-heating the MQ-4 gas sensor which is shown in Figure 3.3. In Figure 3.2, the output voltage increase depends on time and concentration. The methanol fluid is not easy to volatilize. Hence the more the time allowed the more it volatilizes. The MQ-4 gas sensor will be ideal to use it after exposing it to real environment for two days.

The formula of the sensing resistance R_s , of the gas sensor is deduced from the data sheet of MQ-4 gas sensor as shown in equation 3.3. The exposure of the gas to the MQ-4 gas sensor varies its conductivity hence the necessity to characterize it to the suitability of environment. In our characterization the theoretical value was 697.02 mV. In our pre heating process, this value is close after two days of heating. The optimum value in our characterization is 699.00 mV. Methane sensor shares the same character with alcohol sensor, which could be applied only after the same calibration procedure with alcohol sensor. From the research, it can be inferred that the output voltage is almost stable after 48 hours of heating the MQ-4 gas sensor which is shown in figure 3.4. In figure 3.4 the output voltage increase depends on time and concentration. The methanol fluid is not

easy to be volatilized. Hence the more time is allowed the more it volatilizes. After the calculations of the gradients of the best fit lines of all the curves that the curve obtained after 5 minutes exposure time and 2 days heat up time was close to the theoretical value giving equation (4.1) It is within this curve the optimum value of concentration of the gas is obtained so as to be used in the programming of the Arduino (UNO). Comparing with the theoretical equation

$$y = 0.01599x + 697.02 \dots\dots\dots 3.4$$

The gradient percentage error is 1.75%. This may be attributed to: volatilization time and diffusion rate of the gas.

3.3 Infrared sensor results

This section presents results of PIR sensor after conducting to find the optimal values of the height above the ground and horizontal distance for the placement of the PIR sensor to detect intruders. This has been achieved through different placement points and use of people with different heights and walking at different speeds. The results were collected and recorded as tabulated in different tables discussed below. Figures 3.7 to 3.11 show the PIR sensor outputs when walking at difference distances from the PIR sensor for slow, normal and fast walking of the intruders.

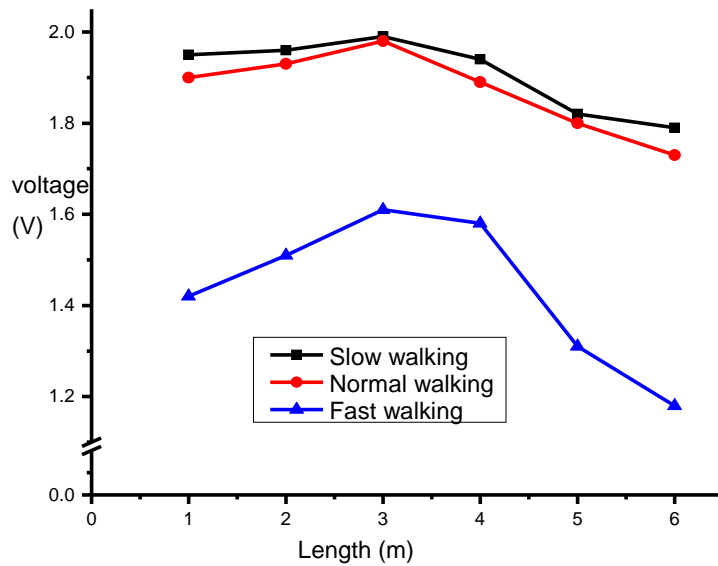


Figure 3.7: The root mean square value of detector voltage at different distances at different walking speed for PIR placed 0.5 m above the ground

In Figure 3.7 detector output for slow and normal walking rates between 1 to 3 meters increase with increase in distance. From 3 to 6 meters the output is inversely proportional to distance. This shows that detector sensitivity and recognition rate is quite high when the object is walking at slow speed and in between 1 to 3 meters. The output of fast walking shows detector sensitivity and recognition rate is quite low. The output of all walking rates decrease from 3 m to 6 m. This show that the detector sensitivity and recognition rate is quite low as the distance increases from 4 meters.

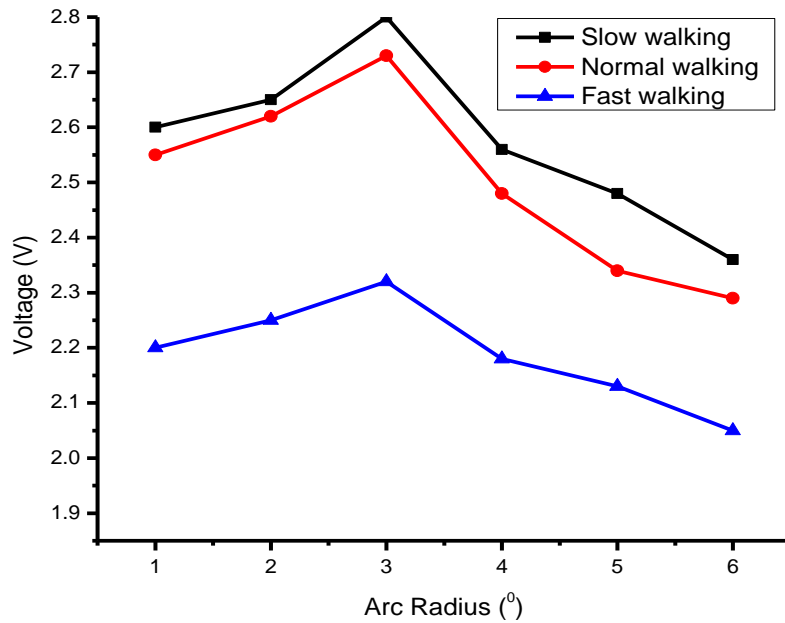


Figure 3.8: The root mean square value of detector voltage at different distances and different walking speed for PIR placed 1.0 m above the ground.

Figure 3.8 shows the output characteristics of the sensor when placed at 1.0 m above the ground. The characteristics of the walking rate curves tend to be similar to the ones of Figure 3.9 but differ with the output values. The detector sensitivity and recognition rate when the sensor is placed at 1-meter height is higher compared to when is placed at 0.5 meters. This may be contributed by the hands movement. The hands are also a source of the infrared radiation hence higher detection.

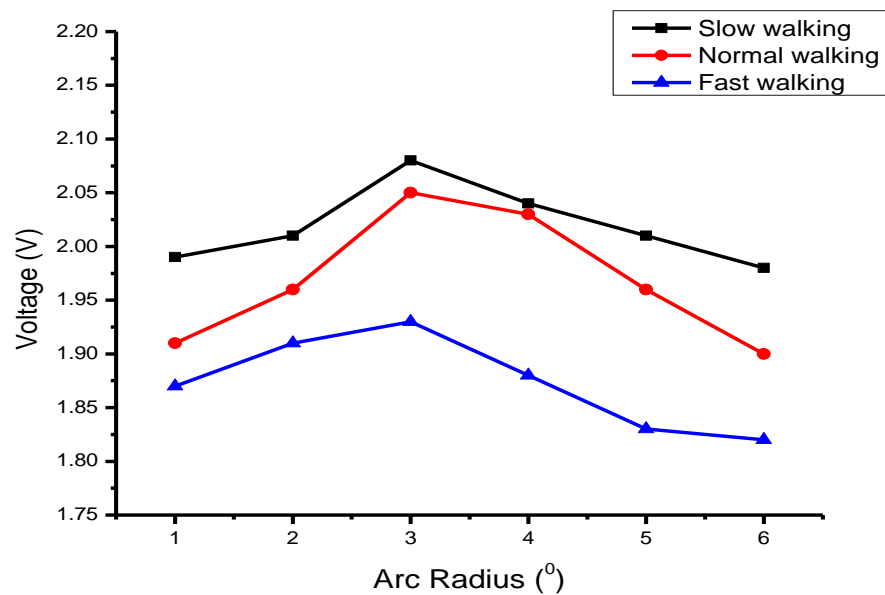


Figure 3.9: The root mean square value of detector voltage at different distances at different walking speed for PIR placed 1.5 m above the ground

Figure 3.9 shows that detector sensitivity and recognition rate is quite high when the object is walking at slow speed and in between 1 to 3 meters for a PIR placed 1.5 m above the ground. The output is higher than when the sensor is placed at 0.5 meters but less than when the sensor is placed at 1.0 meters. This may be attributed to the fact that at 1.5 m fewer body parts are being detected by the PIR sensor.

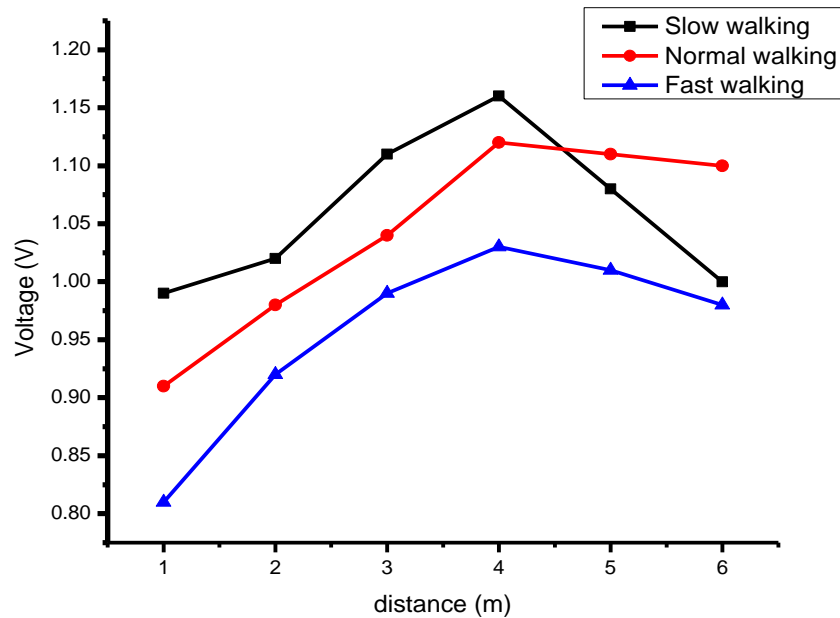


Figure 3.10: The root mean square value of detector voltage at different distances at different walking speed for PIR placed 1.8 m above the ground

The output trend of the sensor placed at 1.8 meters differs with the ones of 0.5, 1.0 and 1.5 meters. This is because it only corresponds to the human head. The detector sensitivity and recognition rate is below 1.2 V hence quite low. The sensitivity for the movements towards and moving away from the detector was tested for slow, normal and fast walking speed.

The PIR output voltage (mV) for different arc radii of motion of intruder when walking towards the PIR sensor at different angles for PIR positioned 0.5 m above the ground.

Figures 3.13 to 3.16 show the output voltages (mV) when walking towards the PIR sensor different angles when the PIR sensor was positioned at 0.5 m, 1.0 m, 1.5 and 1.8 m, respectively above the ground.

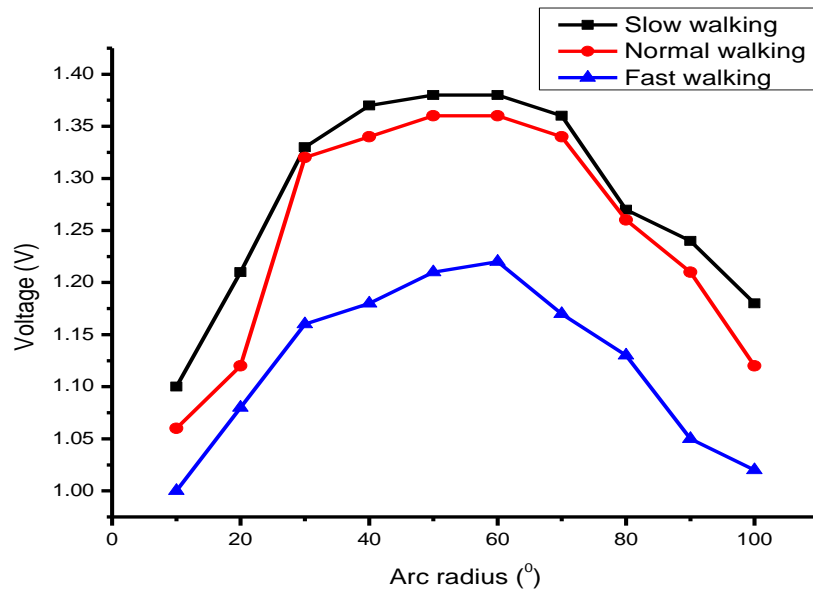


Figure 3.11: Detector sensitivity at different angles when the subject walked towards the detector at different walking speeds sensor placed at 0.5 m above the ground

Figure 3.11 shows that the detector sensitivity is relatively constant from 30° to 70° when the movement is towards the detector at slow and normal walking speed and is quite poor at the extreme ends. The highest output of all walking rates is at 50°. The sensor output is reduced for fast walking speed compared to the normal or slow walking. This is due to minimized interaction between the sources (intruders) of the infrared with the detector.

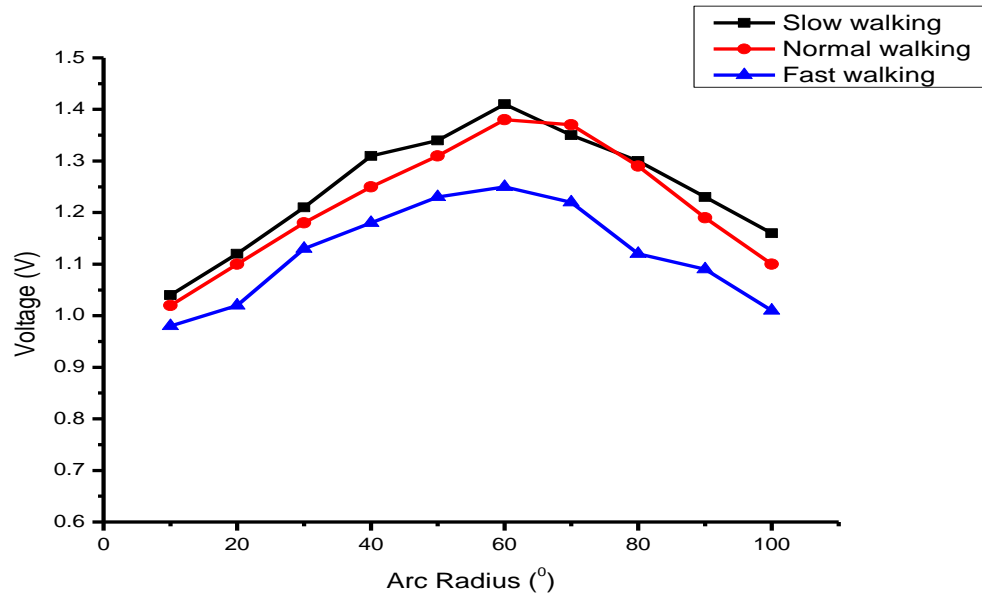


Figure 3.12: Detector sensitivity at different angles when the subject walked towards the detector at different walking speeds sensor placed at 1 m above the ground.

Figure 3.12 shows a steady increase of sensitivity to arc radius of 60° and a drop towards 100°. This shows it is within this angle of 45°-60° that it gives high output signal.

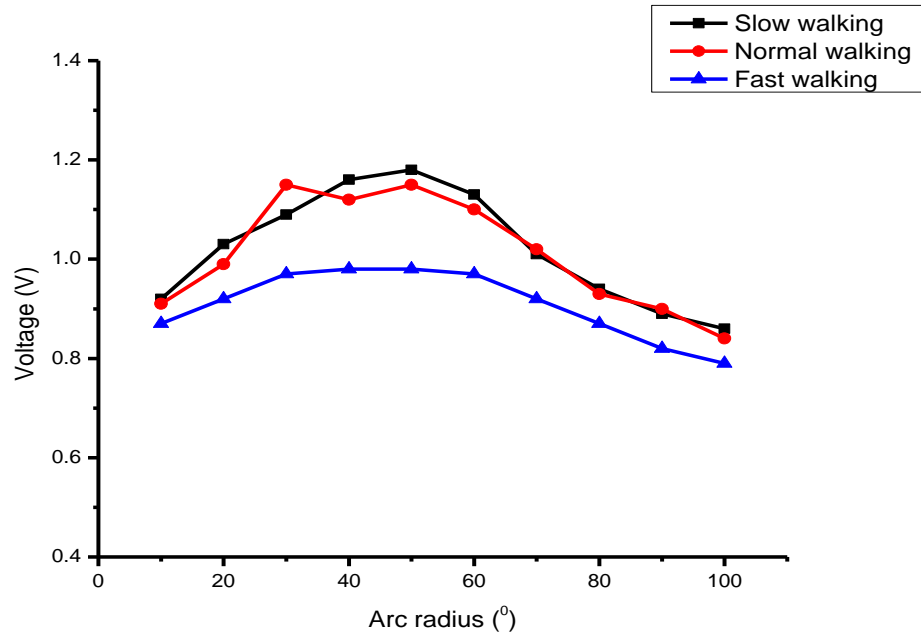


Figure 3.13: Detector sensitivity at different angles when the subject walked towards the detector at different walking speeds sensor placed at 1.5 m.

The sensitivity output seems to be high in between the angle 45° to 60° . The slow walking seems to give the highest output.

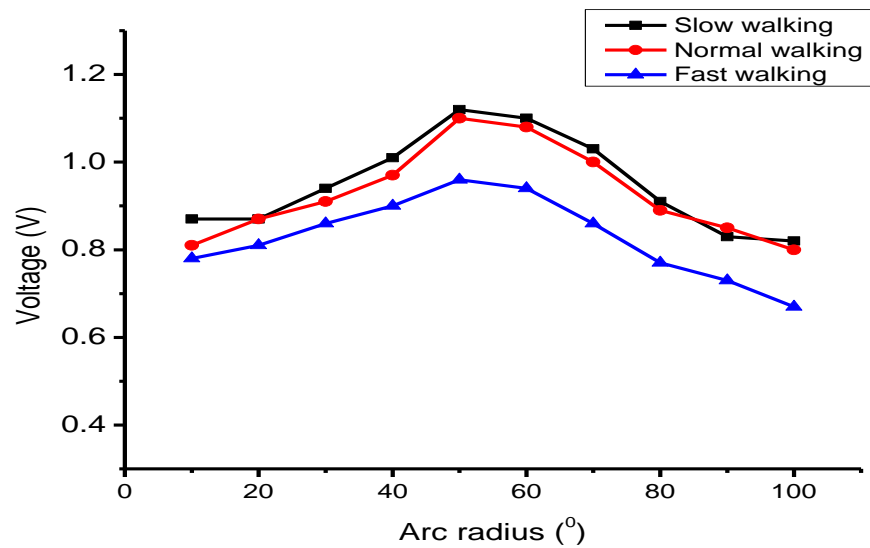


Figure 3.14: Detector sensitivity at different angles when the subject walked towards the detector at different walking speeds sensor placed at 1.8 m.

From Figure 3.13 the sensitivity of the detector decreases. This may be due to the position of the detector above the ground.

Figures 3.15 to 3.18 show the output voltages (mV) when walking away from the PIR sensor at different angles when the PIR sensor was positioned at 0.5 m, 1.0 m, 1.5 and 1.8 m, respectively above the ground.

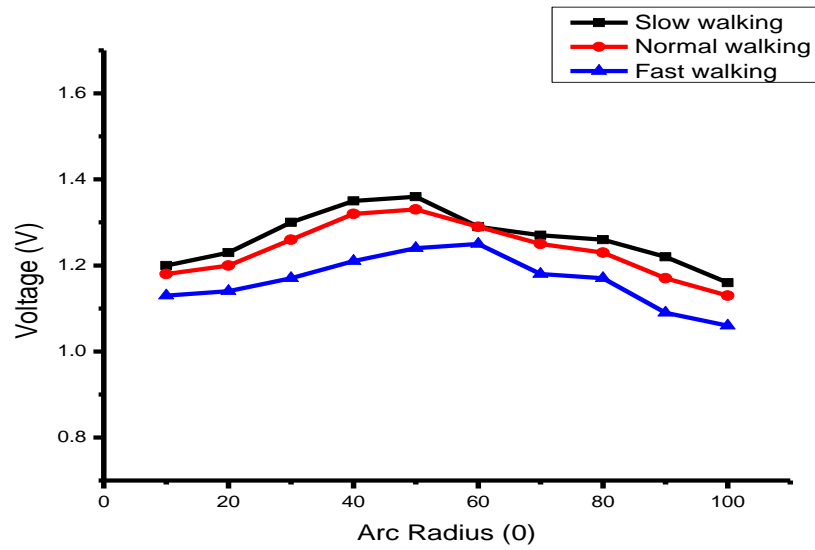


Figure 3.15: Detector sensitivity at different angles when the subject walked away from PIR sensor at different angles with the PIR sensor positioned 0.5 m above the ground.

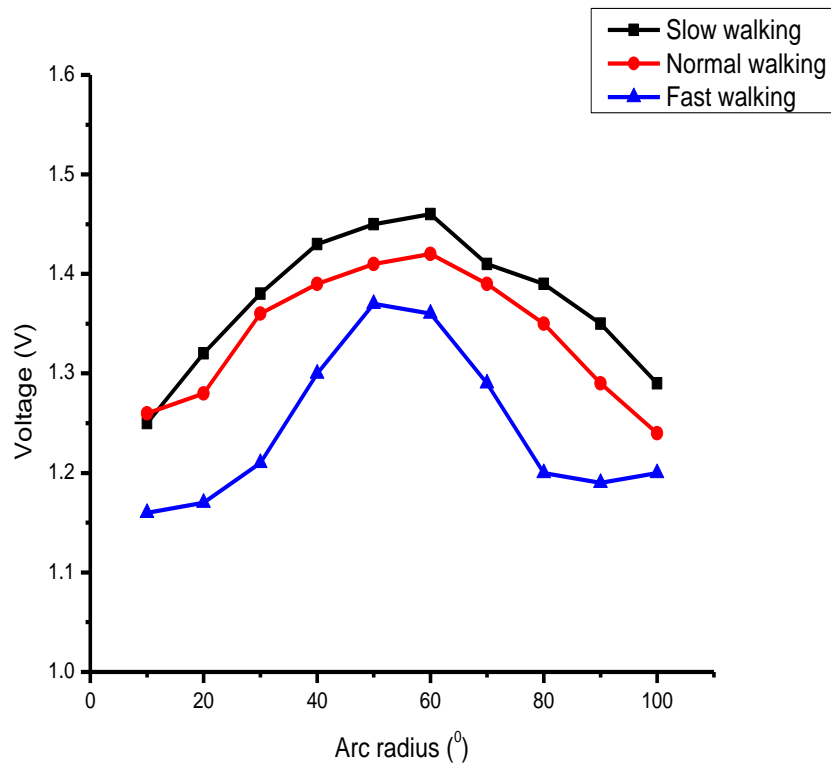


Figure 3.16: Detector sensitivity at different angles when the subject walked away from PIR sensor at different angles with the PIR sensor positioned 1.0 m above the ground.

Figure 3.16 shows the output is higher when the detector is placed at 1.0 m. in addition at slow walking the output is higher than normal and fast walking. This may be attributed by the fact that more interactive time of the radiation and detector is allowed during slow walking.

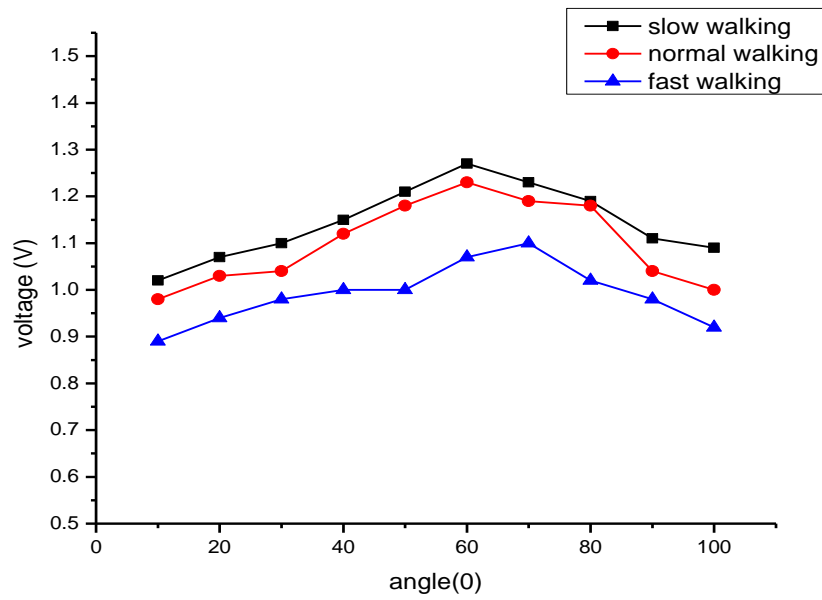


Figure 3.17: Detector sensitivity at different angles when the subject walked away from PIR sensor at different angles with the PIR sensor positioned 1.5 m above the ground.

Figure 3.17 shows the output is slightly less than when it is placed at 1.0 m above the ground. Slow walking also gives more output than normal and fast.

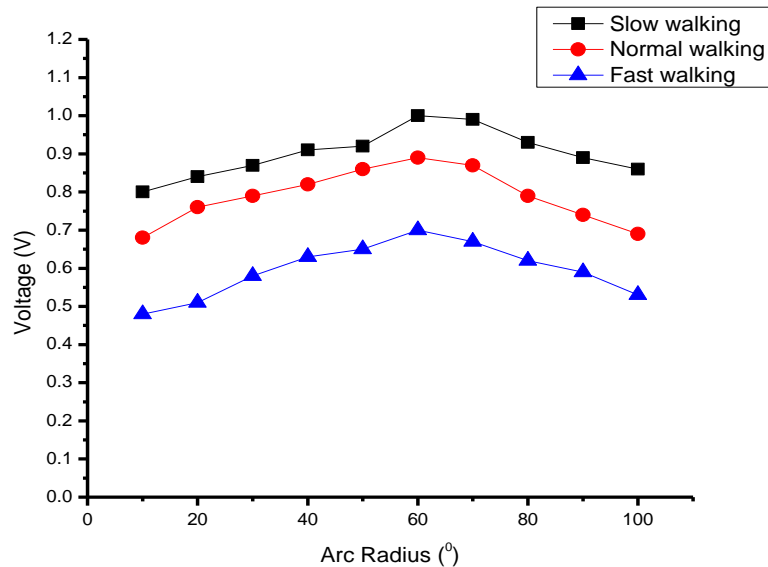


Figure 3.18: Detector sensitivity at different angles when the subject walked away from PIR sensor at different angles with the PIR sensor positioned 1.8 m above the ground.

From figure 3.11 to 3.12 the output voltage increases with the height of the sensor above the ground and is maximum for a distance of 1.0 m (Figure 3.14) and starts to decrease with increase in height.

Generally, from all the graphs the PIR sensor gives higher output during slow walking and is least for fast walking. Comparatively normal walking has higher output compared to the fast walking. From figures 3.15 to 3.18 it can be seen that the output voltage increases as the height of the PIR sensor is increased from 0.5 m (Figure 3.15) a distance of 1.0 m (Figure 3.16) and then decreases to 3.20 been highest at Figure 3.16 when the detector is placed 1.0 m above the ground. Generally the output is higher when the object walks towards than when it walks away. A passive infrared sensor (PIR sensor) being an electronic sensor that measures infrared (IR) light radiating from objects in its field of view. And mostly are used in PIR-based motion detectors. From figures 3.8 to 3.19 shows the trend of increase and decrease of the voltage output when objects walk

away and towards the sensor. The maxima arc radiation range is 55° - 60° . The y-intercept range is below the curves of the walk towards. The maxima output voltage is at 1.46 V which may be attributed to the object direction. In both cases, (object walking away and towards) there is an increase of the voltage output, but the object walking towards is greater than walking away.

3.4 Fire/Temperature Sensor

The LM 35 is an analog linear temperature sensor. The LM35 was connected to the Arduino UNO through the breadboard. The Vcc pin was connected to the 5V pin, the V_{out} was connected to the analogue pins while the GND was also connected to the GND. Table 3.19 shows the temperature against voltage when LM35 was exposed to different temperatures. This data is plotted in the graph of Figure 3.21.

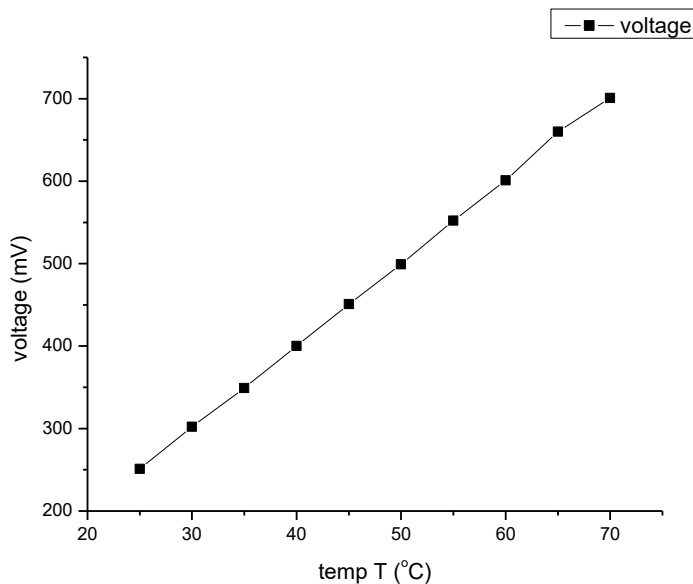


Figure 3.19: A graph of Temperature (°C) against Output voltage (mV) of the LM35 temperature Sensor.

Figure 3.19 shows that the voltage is directly proportional to the temperature change. This is to the fact that the voltage is directly proportional to resistance. Increase in temperature causes more vibrations of molecules of a conductor hence increase in resistance. Temperature is a parameter which has been measured in three major ways: air, ground, and via satellite observation. Most of the fires ignite from temperatures as low as 40 °C. The calibrated temperature sensor threshold was put at 40 °C so as to alert the owner at temperatures above.

3.5 The Integrated Microcontroller Security System

The calibrated sensors were then integrated into the microcontroller as shown in plate 3.1 and 3.2.

Plates 3.1 and 3.2 show all connections of calibrated sensors and outputs to the Arduino Uno microcontroller connected to a power supply. The PIR and MQ-4 sensors were connected to ground (GND) to make the complete circuit.

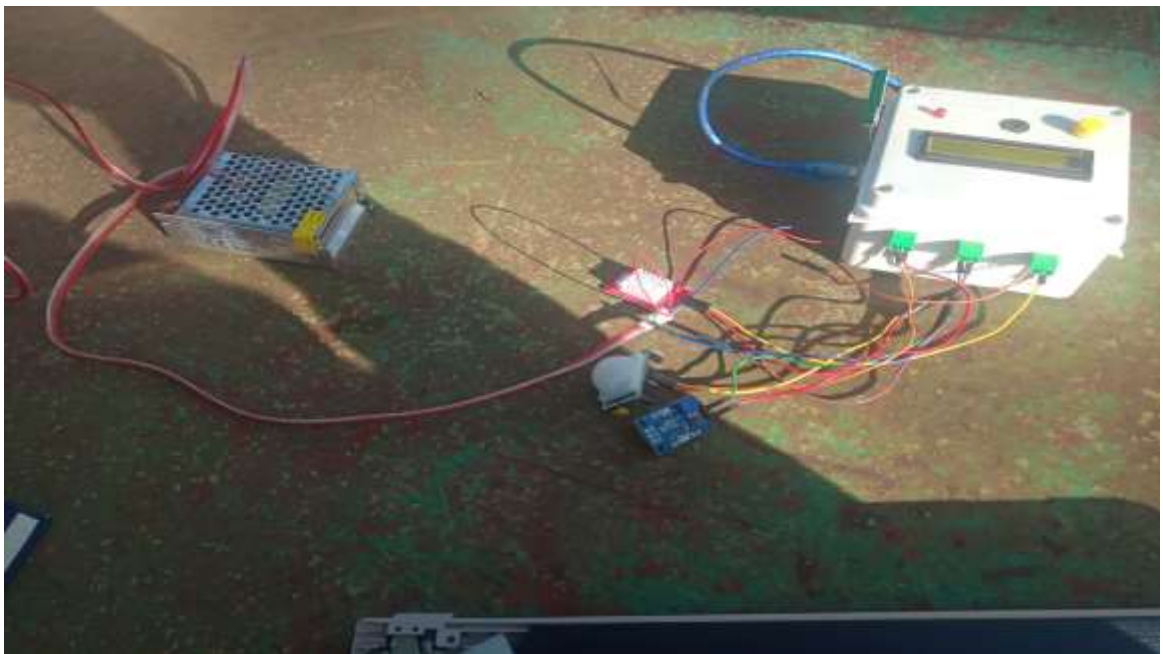


Plate 3.2: MQ-4 gas sensor and the PIR sensor connected to the Arduino UNO.

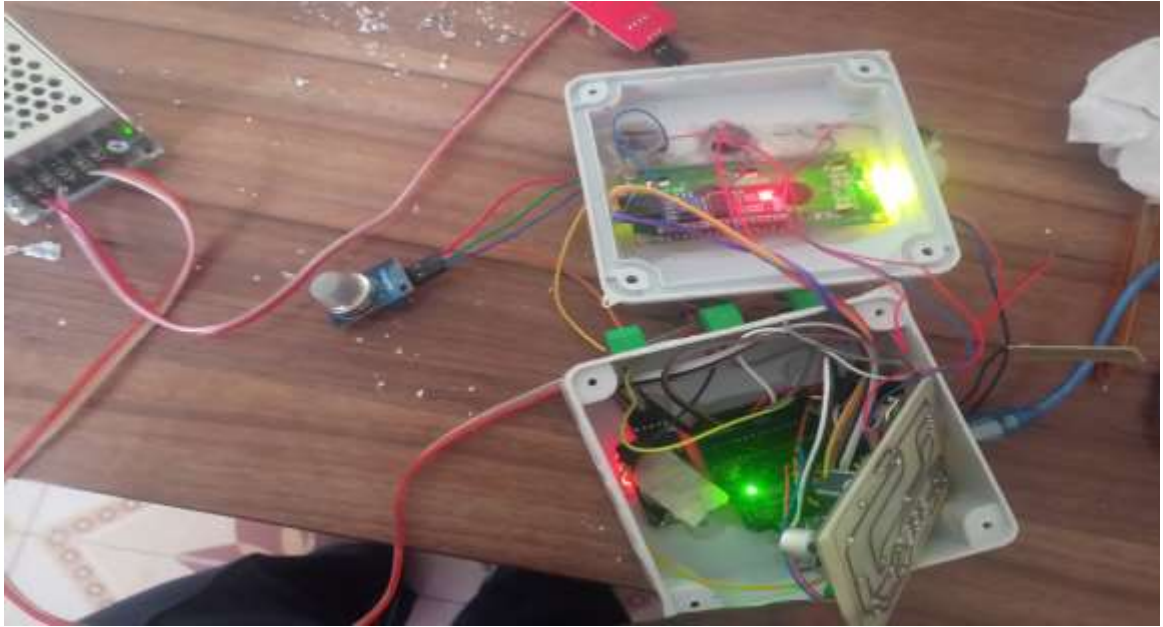


Plate 3.3: The Arduino UNO security system connected to the power supply.

The calibrated gas sensor detected any gas leakage and produced a signal which was fed to the Arduino UNO which compared the gas concentration with an optimal calibrated value. The signal strength was dependent on the concentration of the leaked gas. If the signal is above the optimum value for the MQ-4 gas sensor, the buzzer went on and the owner was alerted through an SMS written 'FIRE'. The gas concentration is then displayed on an LCD display. Sample results obtained are displayed in Plate 3.4 for a gas concentration of 590 ppm, temperature of 28 °C and humidity of 50%. This shows the security conditions are within the normal range therefore no message was sent to the mobile phone.



Plate 3.4: The LCD display when the system under normal conditions of temperature and gas concentration.

When the temperature was above the threshold (40 °C) and the gas concentration was below the concentration threshold, (697 ppm), the buzzer goes ON and the display is shown in Plate 3.5 (a) and message 'FIRE' is sent to the mobile phone number as in Plate 3.5 (b), to warn the home owner.



Plate 3.5: a. The temperature is above 40 °C and the buzzer goes on and the red signal light goes on continuously to indicate there is a danger. b. The short message of fire sent to home owner mobile phone

When an intruder was detected, the PIR sensor signal fed to the Arduino UNO compared the output data with the optimal value of the calibrated sensor. If the value surpassed the optimal value a signal is send to the outputs which alerted the owner in two modes: the buzzer goes ON and a short message written 'INTRUDER' is send to the home owner as shown on Plate 3.6.



Plate 3.6: The picture of short message of intruder send to home owner mobile phone.

The integrated security system of the sensors was able to execute the signal as expected. The gas sensor signal was fed to the Arduino Uno and if the threshold limit was above, the output devices alerted the home owner through raising of an alarm, sending an SMS and displaying it on LCD display. In case of an intruder or fire outbreak the same process of the signal sending would be repeated and the owner alerted.

CHAPTER FOUR

CONCLUSIONS AND RECOMMENDATIONS

4.1 Conclusion

The above calculated variations of the space charge, electric field, and potential energy indicates that the amount of band bending depends only on the surface charges and the concentration of ionized donor atoms or defects hence the concentration of the leaked gas was key if a signal was to surpass the threshold voltage .

The spectrum of a single PIR sensor's temporal signal (analogue feature) is used to represent the human motion features. Decreased sensitivity to walking speeds, is been realized. The higher the speed of the object, the low the output of the signal and vice versa. The coverage area in which the intrusion is suspected to take place the PIR should be placed in such a manner the angles of in between 55° - 60° faces it. Temperature at which the operation of the security system was taking place was monitored. Any fire outbreak alertness was on high percentage of preciseness.

Generally the home security system was functional and the sensors worked at very high precision.

4.3 Recommendations

The home security system has considered only one point of placement of the PIR sensor, where else if more of the PIR sensors can be placed at different points more precise results may be realised. In addition, the placement point the MQ-4 gas sensor is key. The identification performance in the PIR sensor can be improved by increasing spatial sampling frequency.

The temperature sensor may be integrated further with the house fan so as to switch it on to incorporate more aeration. Integration of more sensors to the security system will make it more helpful and reliable to home owners.

REFERENCES

- Agarwal, N., & Nayak, S.G. (2012). Microcontroller based Home Security System with Remote Monitoring, *International Journal of Computer Applications*, 38-41.
- Alkathami, M., Alazzawi L., & Elkateeb A. (2015). Model and Technique analysis of boarder intrusion detection systems. *Global journal of researchers in engineering* 15(7), 1-11
- Celeste, Tholen, (2021). Gate Control Automatic gates, *Smart Home Automation Brigadier Sea l Master*, 755.
- Diarah, R.S., Egbun,e D.O.,& Adedayo, B.A. (2014). Design and Implementation of a Microcontroller Based Automatic Door and Visitors Counter, *International Journal of Scientific Research and Education*, 2, 532–552
- Gwagwa, O.T. (2010). Design and construction of microcontroller mains switch control system, *Master's thesis*, Nnamdi Azikiwe University, Nigeria.
- Hui, T.D. (2013). Microcontroller-based lock using colour security code. *Undergraduate project paper*, University of Malaysia.
- Ichoku, C., & Kaufman Y.J. (2005). A method to derive smoke emission rates from MODIS fire radiative energy measurements, *Geoscience and Remote Sensing, IEEE Transactions*, 43, (11).
- Kaufman, Y.J., Justice, C.O., Flynn, L.P., Kendall, J.D., Prins, E.M., Giglio L., ...& Setzer A.W. (1998). Potential global fire monitoring from EOS-MODIS, *Journal of Geophysical Research*, 103, 10-15

- Kaur, I. (2010). Microcontroller Based Home Automation System with Security, *International Journal of Advanced Computer Science and Applications*, 1(6), 2360-2363
- Kumar, P., & Kumar P. (2013). Arduino based wireless intrusion detection using IR sensor and GSM. *International Journal of computer science and mobile computing*. 2(5), 417-424
- Kaushik, A. R., & Celler, B. G. (2006). Characterization of passive infrared sensors for monitoring occupancy pattern. *Conference proceedings: Annual International Conference of the IEEE Engineering in Medicine and Biology Society. IEEE Engineering in Medicine and Biology Society. Annual Conference, 2006*, 5257–5260. <https://doi.org/10.1109/IEMBS.2006.260207>
- Lakra, P., & Gupta, D.R. (2015). *Microcontroller Based Automatic Control Home Appliances*. Retrieved from <https://www.semanticscholar.org/paper>
- Lau, K.T., & Choo, Y.K. (1989). A microprocessor-based gate security system, *Institute of Electrical and Electronics Engineering Transactions on Consumer Electronics*, 35(4), 858-862.
- Liu, S., Keeler, G. A., Reno, J. L., Sinclair, M. B., & Brener, I. (2016). III–V semiconductor Nano resonators—a new strategy for passive, active, and nonlinear all-dielectric met materials. *Advanced Optical Materials*, 4(10), 1457-1462.
- Luitel, S. (2013). Design and Implementation of a Smart Home System. *Thesis*, Helsinki Metropolia University of Applied Sciences, Finland.
- Moghavvemi, M., and Seng, L. (2004). Pyroelectric infrared sensor for intruder detection in Malaysia. *Department of electrical and Telecommunications*

Engineering. Proceedings of November 21-24, University of Malaysia, Malaysia, 656-659

Murvay, P., & Silea, L. (2012). The state-of-the-art in leak detection and localization methods, *Journal of loss prevention in the process industries*, 25(6):966-973

Nwankwo N., & Nsionu, I., (2013). Design and Implementation of Microcontroller Based Security Door System (Using Mobile Phone & Computer Set), *Journal of Automation and Control Engineering*, 1(1), 65-69

Pregeij, A., & Mozetic, M. (1999). Leak Detection Methods and Defining the Sizes of Leaks. In *the 4th International Conference of Slovenian Society for Nondestructive Testing*, 4(2).

Priya, K.P., Surekha, M., Preethi, R., Devika, T., & Dhivya, N. (2014). Smart Gas Cylinder Using Embedded System, *International Journal of Innovative Research in Electrical, Electronics, Instrumentation and Control Engineering*, 2, 958-962.

Visa, M.I., & Victor, A.A. (2012). Microcontroller Based Anti-theft Security System Using GSM Networks with Text Message as Feedback, *International Journal of Engineering Research and Development*, 2(10), 18-22

Walker, J. (2008). *Fundamentals of Physics*. (8th Ed.). John Wiley and Sons.

Williams, E.W., & Keeling, A.G. (1998). Thick film tin oxide sensors for detecting carbon monoxide at room temperature, *Journal of Materials Science: Materials in Electronics*, 9(1); 51-54.

Zeng, W. (2011). High performance piezoelectric materials and devices for multilayer low temperature cofired ceramic based micro fluids systems. *Ph.D. Thesis*, University of Kentucky, Kentucky.

APPENDICES

Appendix I: The program for running the software for the integrated Arduino microcontroller based security system.

```
program $
#include <SoftwareSerial.h> //GSM
#include<Adafruit_Sensor.h> // Sensors
#include<DHT.h> //DHT
#define DHTPIN 10
#define DHTTYPE DHT22
#include <DS3231.h> // RTC
#include <LiquidCrystal_I2C.h> //LCD

SoftwareSerial mySerial(3, 2); //GSM pins

DHT dht (DHTPIN, DHTTYPE);
LiquidCrystal_I2C lcd(0x27,16,2);
DS3231 rtc(SDA, SCL);
Time t;
#define pirPin 8

int calibrationTime = 30; // Calibration
long unsigned int lowIn;
long unsigned int pause = 5000;
boolean lockLow = true;
boolean takeLowTime;
int PIRValue = 0;

byte degree[8]={
  0b00110,
  0b01001,
  0b01001,
  0b01001,
  0b00010,
  0b00000,
  0b00000,
  0b00000,
  0b00000,
  0b00000;

int buzzer = 9;
int smokeAO = A0;
int sensorThres = 400;
int T;
int H;
int waitTime = 2;// in minutes

int measurePin = 0;

//Define Time
unsigned long int hhour = 0;
unsigned long int mmin = 0;
unsigned long int ssec = 0;
unsigned long int ttime = 0;
unsigned long int wait1 = 0;

String incomingData; // for storing incoming serial data
String message = ""; // A String for storing the message
```

```

int smokeVal = analogRead(SMOKEAU);
T=dht.readTemperature();
H=dht.readHumidity();
lcd.clear();
lcd.setCursor(8, 0);
lcd.print(rtc.getTimeStr());

lcd.setCursor(0,1);
lcd.print("T:");
lcd.print(T);
lcd.write(byte(0));
lcd.print("C");

lcd.setCursor(7,1);
lcd.print("H:");
lcd.print(H);
lcd.print("%");

lcd.setCursor(0,0);
lcd.print("G:");
lcd.print(smokeVal);

lcd.print(" ");

```

```

Serial.print(rtc.getDateStr());
Serial.print(",");

```

```

Serial.print(rtc.getDateStr());
Serial.print(",");
Serial.print(rtc.getTimeStr());
Serial.print(",");

```

```

Serial.print("T:");
Serial.print(T);
Serial.write(byte(0));
Serial.print("C");
Serial.print(",");
Serial.print("H:");
Serial.print(H);
Serial.print("%");
Serial.print(",");
Serial.print("G:");
Serial.print(smokeVal);
Serial.print("ppm");
Serial.print(",");
Serial.print(ttime);
Serial.println();

```


```

if (smokeVal > sensorThres){
    digitalWrite(buzzer,HIGH);
    send_message("Fire");
}
else{
    digitalWrite(buzzer,LOW);

```

```
-  
    if (smokeVal > sensorThres){  
        digitalWrite(buzzer,HIGH);  
        send_message("Fire");  
    }  
    else{  
        digitalWrite(buzzer,LOW);  
    }  
  
    |  
    t = rtc.getTime();  
    hhour = t.hour;  
    mmin = t.min;  
    ssec = t.sec;  
    ttime = (hhour * 60) + mmin;  
    wait1 = ttime % waitTime;  
  
    delay(1000);  
  
}
```

```
void loop() {  
  
}
```



```
PIRValue = 0;
lockLow = true;
Serial.println("Motion ended.");
message = "Motion ended.";
send_message(message);
delay(50);
}
}
}
```

```
void send_message(String message)
{
  mySerial.println("AT+CMGF=1");
  delay(100);
  mySerial.println("AT+CMGS=\"+254727092216\"");
  delay(100);
  mySerial.println(message);
  delay(100);
  mySerial.println((char)26);
  delay(100);
  mySerial.println();
  delay(1000);
}
```

Appendix II: List of Publications

1. Sakayo N.M., Mutuku J.N and Ngaruiya J.M. (2019). Design and Calibration of a Microcontroller Based MQ-4 Gas Sensor for Domestic Cooking Gas System. *SSRG International Journal of Applied Physics (SSRG-IJAP)*, (6): 2.
2. Sakayo N.M., Mutuku J.N and Ngaruiya J.M. (2019). Design and Calibration of a Microcontroller Based Passive Infrared Sensor for Domestic Intruder Detection. *International Journal of Innovative Research in Science, Engineering and Technology (IJIRSET)*, (9):6.